

Nonconvex piecewise linear functions: Advanced formulations and simple modeling tools

Joey Huchette

Department of Computational and Applied Mathematics, Rice University, joehuchette@rice.edu

Juan Pablo Vielma

Sloan School of Management, Massachusetts Institute of Technology, jvielma@mit.edu

We present novel mixed-integer programming (MIP) formulations for optimization over nonconvex piecewise linear functions. We exploit recent advances in the systematic construction of MIP formulations to derive new formulations for univariate functions using a geometric approach, and for bivariate functions using a combinatorial approach. All formulations are strong, small (so-called *logarithmic* formulations), and have other desirable computational properties. We present extensive experiments in which they exhibit substantial computational performance improvements over existing approaches. To accompany these advanced formulations, we present `PiecewiseLinearOpt`, an extension of the JuMP modeling language in Julia that implements our models (alongside other formulations from the literature) through a high-level interface, hiding the complexity of the formulations from the end-user.

Key words: Piecewise linear, Integer programming

1. Introduction

Consider a piecewise linear function $f : D \rightarrow \mathbb{R}$, where $D \subseteq \mathbb{R}^n$. That is, f can be described by a partition of the domain D into a finite family $\{C^i\}_{i=1}^d$ of polyhedral pieces, where for each piece C^i there is an affine function $f^i : C^i \rightarrow \mathbb{R}$ such that $f(x) = f^i(x)$ for all $x \in C^i$. In this work, we will study methods to solve optimization problems containing piecewise linear functions. This encompasses cases where f appears either in the objective function (e.g. $\min_x f(x)$), or in a constraint (e.g. the feasible domain for the optimization problem is partially defined by the inequality $f(x) \leq 0$).

The potential applications for this class of optimization problems are legion. Piecewise linear functions arise naturally throughout operations (Croxtton et al. 2003, 2007, Liu and Wang 2015) and engineering (Fügenschuh et al. 2014, Graf et al. 1990, Silva et al. 2012). They are a natural

choice for approximating nonlinear functions, as they often lead to optimization problems that are easier to solve than the original problem (Bergamini et al. 2005, 2008, Castro and Teles 2013, Geißler et al. 2012, Kolodziej et al. 2013, Misener et al. 2011, Misener and Floudas 2012). For example, there has been recently been significant interest in using piecewise linear functions to approximate complex nonlinearities arising in gas network optimization (Cudas and Camponogara 2012, Cudas et al. 2012, Martin et al. 2006, Mahlke et al. 2010, Misener et al. 2009, Silva and Camponogara 2014); see Koch et al. (2015) for a recent book on the subject.

If the function f happens to be convex, it is possible to reformulate our optimization problem into an equivalent linear programming (LP) problem (provided that D is polyhedral). However, if f is nonconvex, this problem is NP-hard in general (Keha et al. 2006). A number of specialized algorithms for solving piecewise linear optimization problems have been proposed over the years (Beale and Tomlin 1970, de Farias Jr. et al. 2008, 2013, Keha et al. 2006, Tomlin 1981). Another popular approach is to use mixed-integer programming (MIP) to encode the logical constraints $x \in C^i \implies f(x) = f^i(x)$ using auxiliary integer decision variables. There are many possible ways to do this, and the MIP approach to modeling optimization problems containing piecewise linear functions has been an active and fruitful area of research for decades (Balakrishnan and Graves 1989, Croxton et al. 2003, D’Ambrosio et al. 2010, Dantzig 1960, Jeroslow and Lowe 1984, 1985, Keha et al. 2004, Lee and Wilson 2001, Magnanti and Stratila 2004, Markowitz and Manne 1957, Padberg 2000, Sherali and Wang 2001, Vielma and Nemhauser 2011, Vielma et al. 2010, Wilson 1998). This line of work has produced a large number of MIP formulations that exploit the high performance and flexibility of modern MIP solvers (Bixby and Rothberg 2007, Jünger et al. 2010), with varying degrees of success. The 2010 *Operations Research* paper of Vielma et al. (2010) compiled these formulations into a unified framework and provided extensive comparisons of their computational performance. Notably, they showcase the substantial computational advantage of *logarithmic* formulations (Vielma and Nemhauser 2011), so-called because their size scales logarithmically in the number of piecewise segments. This work has subsequently sparked attempts to

construct logarithmic formulations for other nonconvex constraints (Huchette and Vielma 2019a, Huchette et al. 2017, Vielma 2018). However, the complexity of the logarithmic formulations has resulted in a relatively low rate of adoption in practice, despite their computational efficacy.

In this paper, we study piecewise linear functions as a case study for recent developments in the systematic construction of advanced MIP formulations for nonconvex structures. We present novel logarithmic formulations for piecewise linear functions that improve on the state-of-the-art, and also provide accessible software modeling tools that hide the resulting complexity of these formulations from end users. Specifically, the main contributions of this paper are:

1. **For univariate functions: A speed-up of up to 3x on harder instances.** In Section 3 we present new formulations for univariate piecewise linear functions that preserve the size and strength of the existing logarithmic formulations, while significantly improving their branching behavior. We show how these formulations computationally outperform the crowded field of existing formulations. In particular, we focus on regimes that are known to be problematic for existing formulations, and observe an improvement of up to 3x on harder instances, though the magnitude of improvement varies among different solvers. To accomplish this, we adapt the geometric formulation construction technique of Vielma (2018) to develop an unorthodox MIP formulation that exploits general integer (rather than binary) variables. We believe that our results suggest that general integer formulations are a fruitful direction for future MIP formulation research.

2. **For bivariate functions: An order-of-magnitude speed-up.** In Section 4 we study bivariate piecewise linear functions with generic grid triangulated domains, extending and applying the combinatorial formulation construction technique of Huchette and Vielma (2019a) to develop several families of novel logarithmic formulations. Along the way, we show that for the disjunctive constraints considered in this work (the vast class of “combinatorial disjunctive constraints” (Huchette and Vielma 2019a)), the common loss of strength resulting from intersecting MIP formulations is entirely avoided (Theorem 2). Finally, we show that the formulations we derive offer a significant computational advantage over existing techniques.

3. An accessible modeling library for advanced formulations. In Section 5, we present a `PiecewiseLinearOpt`, an extension of the JuMP algebraic modeling language (Dunning et al. 2017) that offers a high-level way to model piecewise linear functions in practice. The package supports all the MIP formulations for piecewise linear functions discussed in this work, and generates them automatically and transparently from the user. We believe that easy-to-use modeling interfaces such as `PiecewiseLinearOpt` are crucial for the practical adoption of advanced MIP formulations like those presented in this work.

2. Piecewise linear functions and combinatorial disjunctive constraints

Consider a continuous¹ piecewise linear function $f : D \rightarrow \mathbb{R}$, where $D \subset \mathbb{R}^n$ is bounded. We will describe f in terms of the domain pieces $\{C^i \subseteq D\}_{i=1}^d$ and affine functions $\{f^i\}_{i=1}^d$ as above; we assume that the pieces cover the domain D and that their interiors do not overlap. Furthermore, we assume that our function $f : \mathbb{R}^n \rightarrow \mathbb{R}$ is *non-separable* and cannot be decomposed as the sum of lower-dimensional piecewise linear functions. This is without loss of generality, as if such a decomposition exists, we could apply our formulation techniques to the individual pieces separately. Finally, we will focus primarily on the regime where the dimension n of the domain is relatively small: when f is either univariate ($n = 1$) or bivariate ($n = 2$) with a grid triangulated domain; see Figure 1 for an illustrative example of each. Low dimensional piecewise linear functions are broadly applicable (especially with the non-separability assumption), and are sufficiently complex to warrant in-depth analysis. We tabulate notation we will use for the remainder in Table 1.

In order to solve an optimization problem containing f , we will construct a formulation for its graph $\mathbf{gr}(f) \stackrel{\text{def}}{=} \{(x, f(x)) \mid x \in D\}$, which will couple the argument x with the function output $f(x)$. We can view the graph disjunctively as the union $\mathbf{gr}(f) = \bigcup_{i=1}^d S^i$, where each $S^i = \{(x, f^i(x)) \mid x \in C^i\}$ is a *segment* of the graph.

EXAMPLE 1. Consider the univariate piecewise linear function $f : [1, 5] \rightarrow \mathbb{R}$ with the domain pieces $C^1 = [1, 2]$, $C^2 = [2, 3]$, $C^3 = [3, 4]$, and $C^4 = [4, 5]$, where

$$x \in C^1 \implies f(x) = 4x - 4, \quad x \in C^2 \implies f(x) = 3x - 2, \quad (1a)$$

$$x \in C^3 \implies f(x) = 2x + 1, \quad x \in C^4 \implies f(x) = x + 5. \quad (1b)$$

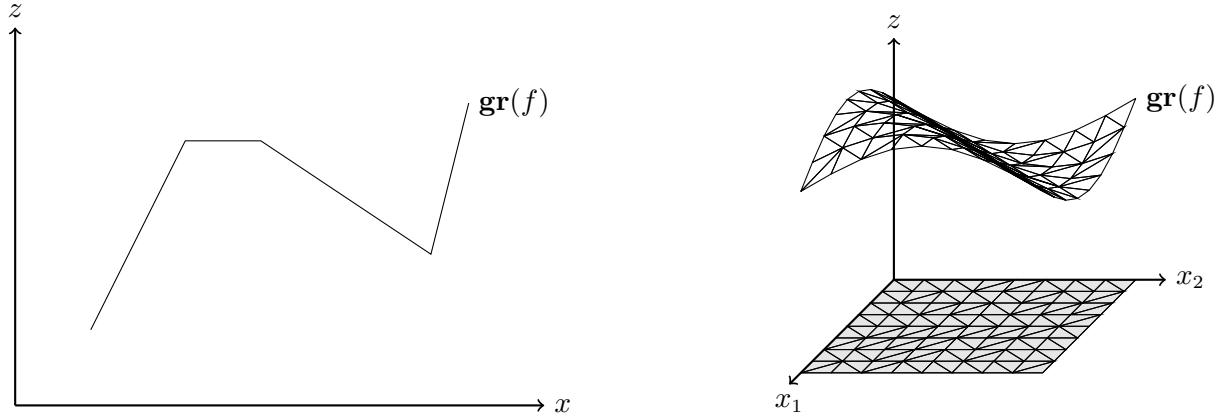


Figure 1 (Left) A univariate piecewise linear function, and (Right) a bivariate piecewise linear function with a grid triangulated domain.

Notation	Formal Definition	Description
$\llbracket d \rrbracket$	$\{1, \dots, d\}$	All integers from 1 to d
$\mathbb{R}_{\geq 0}^n$	$\{x \in \mathbb{R}^n \mid x \geq 0\}$	Nonnegative orthant in n -dimensional space
Δ^V	$\{\lambda \in \mathbb{R}_{\geq 0}^V \mid \sum_{v \in V} \lambda_v = 1\}$	Unit simplex on ground set V
$\text{supp}(\lambda)$	$\{v \in V \mid \lambda_v \neq 0\}$	Nonzero values (<i>support</i>) of λ
$P(T)$	$\{\lambda \in \Delta^V \mid \text{supp}(\lambda) \subseteq T\}$	Face of the unit simplex given by components T
$\text{ext}(P)$	-	Extreme points of polyhedra P
$\text{gr}(f)$	$\{(x, f(x)) \mid x \in \text{dom}(f)\}$	Graph of the function f
$[V]^2$	$\{\{u, v\} \in V \times V \mid u \neq v\}$	All unordered pairs of elements in V
$\text{Em}(\mathcal{T}, H)$	$\bigcup_{i=1}^d P(T^i) \times \{H_i\}$	Embedding of disjunctive constraint (where H_i is the i -th row of H)
$\text{Conv}(S)$	-	Convex hull of S
$Q(\mathcal{T}, H)$	$\text{Conv}(\text{Em}(\mathcal{T}, H))$	Convex hull of embedding
$\text{aff}(H)$	-	Affine hull of the rows of H
$L(H)$	$\{y - H_1 \mid y \in \text{aff}(H)\}$	Linear space parallel to the affine hull $\text{aff}(H)$ (where H_1 is first row of H)
$M(b)$	$\{y \in L(H) \mid b \cdot y = 0\}$	The hyperplane in $L(H)$ normal to b
$\text{Vol}(D)$	-	Volume of set D
$A * B$	$\{\{u, v\} \mid u \in A, v \in B\}$	Unordered pairs of elements in A and B

Table 1 Notation used throughout the paper.

The graph of the piecewise linear function is then

$$\text{gr}(f) = \{(x, 4x - 4) \mid x \in C^1\} \cup \{(x, 3x - 2) \mid x \in C^2\} \cup \{(x, 2x + 1) \mid x \in C^3\} \cup \{(x, x + 5) \mid x \in C^4\}.$$

Similarly, we take the bivariate piecewise linear function $g : [0, 1]^2 \rightarrow \mathbb{R}$ with the domain partition

$$C^1 = \{x \in [0, 1]^2 \mid x_1 \leq x_2\} \text{ and } C^2 = \{x \in [0, 1]^2 \mid x_1 \geq x_2\}, \text{ and}$$

$$x \in C^1 \implies g(x) = -x_1 + 3x_2 + 1, \quad x \in C^2 \implies g(x) = x_1 + x_2 + 1. \quad (2)$$

The corresponding graph is

$$\text{gr}(g) = \{(x_1, x_2, -x_1 + 3x_2 + 1) \mid x \in C^1\} \cup \{(x_1, x_2, x_1 + x_2 + 1) \mid x \in C^2\}.$$

We refer the reader to [Vielma et al. \(2010\)](#) for an exhaustive taxonomy of existing MIP formulations for piecewise linear functions. In this work, we will build formulations for piecewise linear functions using the *combinatorial disjunctive constraint* approach ([Huchette and Vielma 2019a](#)).

Given a piecewise linear function, take the family of sets $\mathcal{T} = (T^i = \text{ext}(C^i))_{i=1}^d$ corresponding to the extreme points of each piece of the domain C^i . This describes the underlying combinatorial structure among the segments of the graph, induced by the shared breakpoints over the ground set $V = \bigcup_{i=1}^d T^i$. Define $\Delta^V \stackrel{\text{def}}{=} \{ \lambda \in \mathbb{R}_{\geq 0}^V \mid \sum_{v \in V} \lambda_v = 1 \}$ as the standard simplex, $\text{supp}(\lambda) \stackrel{\text{def}}{=} \{ v \in V \mid \lambda_v \neq 0 \}$ as the nonzero values (*support*) of λ , and $P(T) \stackrel{\text{def}}{=} \{ \lambda \in \Delta^V \mid \text{supp}(\lambda) \subseteq T \}$ as the face of the standard simplex with support restricted to T . Then we can express the graph in terms of \mathcal{T} as $\mathbf{gr}(f) = \left\{ \sum_{v \in V} \lambda_v (v, f(v)) \mid \lambda \in \bigcup_{i=1}^d P(T^i) \right\}$. In particular, we can build a formulation for f through the *combinatorial disjunctive constraint* $\lambda \in \bigcup_{i=1}^d P(T^i)$ ([Huchette and Vielma 2019a](#)), which is a disjunctive constraint on convex multipliers λ where each alternative $P(T^i)$ is some face of the unit simplex Δ^V .

EXAMPLE 2. Take f as given in Example 1. The graph of this function has $d = 4$ segments, and the breakpoints between segments are given by the set $V = \llbracket d + 1 \rrbracket$. We have that $(x, z) \in \mathbf{gr}(f)$ if and only if $(x, z) = \sum_{v \in V} (v, f(v)) \lambda_v$ for some $\lambda \in \bigcup_{i=1}^4 P(\{i, i + 1\})$.

Similarly, for the function g as in Example 1, we can take $V = \{0, 1\}^2$ and observe that $(x, z) \in \mathbf{gr}(g)$ if and only if $(x, z) = \sum_{v \in V} (v, f(v)) \lambda_v$ for some $\lambda \in P(\{(0, 0), (1, 0), (1, 1)\}) \cup P(\{(0, 0), (0, 1), (1, 1)\})$.

For the remainder, we assume without loss of generality (w.l.o.g.) that $V = \llbracket d + 1 \rrbracket$ for univariate functions. We also note that the constraint $\lambda \in \bigcup_{i=1}^{d+1} P(\{i, i + 1\})$ from Example 2 is the classical special ordered set of type 2 (SOS2) constraint ([Beale and Tomlin 1970](#)). Additionally, we will restrict our attention to bivariate functions with *grid triangulated* domains; that is, the domain of the function is a rectangle in \mathbb{R}^2 decomposed according to a regular grid, and that each subrectangle within that decomposition is partitioned into exactly two triangular domain pieces. In this setting, we may assume w.l.o.g. and that $V = \llbracket d_1 + 1 \rrbracket \times \llbracket d_2 + 1 \rrbracket$ for bivariate functions.

The logarithmic formulations of Vielma and Nemhauser (2011) apply to several special classes of combinatorial disjunctive constraints, including SOS2 constraints. These logarithmic formulations have been observed to perform extremely well computationally; this can be largely attributed to their strength and size. With regards to strength, the formulations are *ideal*: their LP relaxations offer the tightest possible convex relaxation for the underlying nonconvex set $\mathbf{gr}(f)$, and their extreme points naturally satisfy the desired integrality condition (see Vielma (2015) for more about formulation strength). Moreover, the formulations are small, as the number of auxiliary variables and (general inequality) constraints scale logarithmically in the number of segments of the piecewise linear functions. The novel formulations presented in this work will also possess these two properties. Moreover, we will also design them to have other desirable computational properties (univariate functions in Section 3), and such that they apply to a much larger class of piecewise linear functions than previously considered (bivariate functions in Section 4). To achieve this, we use and extend two recent generalizations of Vielma and Nemhauser (2011): the geometric *embedding formulation* technique of Vielma (2018), and the combinatorial *independent branching formulation* technique of Huchette and Vielma (2019a). When applied to the SOS2 constraint, these techniques yield two formulations we denote the *logarithmic embedding* (LogE) and the *logarithmic independent branching* (LogIB) formulations, respectively. Both formulations are quite similar; however, while LogIB always exactly coincides with the original logarithmic formulation of Vielma and Nemhauser (2011), LogE only does so when d is a power-of-two (Muldoon 2012) (we provide an example of this divergence in Appendix B). These two formulations will serve as the reference benchmark formulation in our computational experiments.

3. Formulations for univariate piecewise linear functions

In this section we will adapt a geometric formulation construction method to build novel strong logarithmic formulations for univariate piecewise linear functions.

3.1. The embedding approach

The embedding approach of Vielma (2018) provides one way to construct strong formulations for disjunctive constraints. To formulate $\bigcup_{i=1}^d P(T^i)$, assign each alternative $P(T^i)$ a unique integer

code $H_i \in \mathbb{Z}^r$. We call the collection of all codes as rows in a matrix $H \in \mathbb{Z}^{d \times r}$ an *encoding*, where H_i is the i -th row of H . Then the disjunctive set is “embedded” in a higher-dimensional space as $\text{Em}(\mathcal{T}, H) \stackrel{\text{def}}{=} \bigcup_{i=1}^d (P(T^i) \times \{H_i\})$. In the case studied by Vielma (2018) where $H \in \{0, 1\}^{d \times r}$ is a binary encoding, this easily leads to a MIP formulation for $\bigcup_{i=1}^d P(T^i)$. However, we will be interested in constructing formulations using general integer encodings, which requires some care to ensure that the embedding leads to a valid formulation.

DEFINITION 1. Take the matrix $H \in \mathbb{Z}^{d \times r}$, and the collection of its rows as $\Lambda = \{H_i\}_{i=1}^d$.

- H is in *convex position* if $\text{ext}(\text{Conv}(\Lambda)) = \Lambda$.
- H is *hole-free* if $\text{Conv}(\Lambda) \cap \mathbb{Z}^r = \Lambda$.

Take $\mathcal{H}_r(d) \stackrel{\text{def}}{=} \{H \in \mathbb{Z}^{d \times r} \mid H \text{ is hole-free and in convex position, and each } H_i \text{ is distinct}\}$.

The following straightforward extension of Proposition 1 and Corollary 1 in Vielma (2018) shows that encodings in $\mathcal{H}_r(d)$ always lead to valid formulations.

PROPOSITION 1. Take the family of sets $\mathcal{T} = (T^i \subseteq V)_{i=1}^d$, along with $r \geq \lceil \log_2(d) \rceil$ and $H \in \mathcal{H}_r(d)$. Then $Q(\mathcal{T}, H) \stackrel{\text{def}}{=} \text{Conv}(\text{Em}(\mathcal{T}, H))$ is a rational polyhedron, and an ideal formulation for $\bigcup_{i=1}^d P(T^i)$ is $\{(\lambda, y) \in Q(\mathcal{T}, H) \mid y \in \mathbb{Z}^r\}$. We call this the embedding formulation of \mathcal{T} associated to H .

In general, constructing a linear inequality description of $Q(\mathcal{T}, H)$ is difficult, the resulting representation may be exponentially large, and its structure is highly dependent on the interplay between the sets \mathcal{T} and the encoding H . Fortunately, (Vielma 2018, Proposition 2) gives an explicit description of $Q(\mathcal{T}, H)$ for the SOS2 constraint with any choice of binary encoding H . This description is geometric, in terms of the difference directions $H_{i+1} - H_i$ between adjacent codes. In particular, we will need to compute all hyperplanes $M(b) \stackrel{\text{def}}{=} \{y \in L(H) \mid b \cdot y = 0\}$ spanned by these difference directions in $L(H) \stackrel{\text{def}}{=} \{y - H_1 \mid y \in \text{aff}(H)\}$, the linear space parallel to the affine hull of H . The following straightforward extension of Proposition 2 from Vielma (2018) shows that this description also holds for any encoding in $\mathcal{H}_r(d)$.

PROPOSITION 2. Take $H \in \mathcal{H}_r(d)$, along with $H_0 \equiv H_1$ and $H_{d+1} \equiv H_d$ for notational convenience. Let $\mathcal{B} \subset L(H) \setminus \{\mathbf{0}^r\}$ be normal directions such that $\{M(b)\}_{b \in \mathcal{B}}$ is the set of hyperplanes spanned by

$\{H_{i+1} - H_i\}_{i=1}^{d-1}$ in $L(H)$. If $\mathcal{T} = (\{i, i+1\})_{i=1}^d$ is the family of sets defining the SOS2 constraint on $d+1$ breakpoints, then $Q(\mathcal{T}, H)$ is equal to all $(\lambda, y) \in \Delta^{d+1} \times \text{aff}(H)$ such that

$$\sum_{v=1}^{d+1} \min\{b \cdot H_{v-1}, b \cdot H_v\} \lambda_v \leq b \cdot y \leq \sum_{v=1}^{d+1} \max\{b \cdot H_{v-1}, b \cdot H_v\} \lambda_v \quad \forall b \in \mathcal{B}.$$

Consider the class of encodings $K^r \in \mathcal{H}_r(d)$ for $r = \lceil \log_2(d) \rceil$ known as Gray codes (Savage 1997), where adjacent codes differ in exactly one component (i.e. $\|K_{j+1}^r - K_j^r\|_1 = 1$ for all $j \in \llbracket d-1 \rrbracket$). This class of encodings enjoys the desirable property that the spanning hyperplanes needed for Proposition 2 are parsimonious and simple to describe in closed form. For the remainder, we will work with a particular Gray code known as the binary reflected Gray code (BRGC); see Appendix A for a formal definition.

We can construct the *logarithmic embedding* (LogE) formulation for the SOS2 constraint due to Vielma (2018) by applying Proposition 2 with the BRGC. This formulation is ideal, and its size scales logarithmically in the number of segments d .

EXAMPLE 3. The LogE formulation for the SOS2 constraint with $d = 4$ (arising in (1)) is:

$$\lambda_3 \leq y_1, \quad \lambda_1 + \lambda_5 \leq 1 - y_1, \quad \lambda_4 + \lambda_5 \leq y_2, \quad \lambda_1 + \lambda_2 \leq 1 - y_2, \quad (\lambda, y) \in \Delta^V \times \{0, 1\}^2. \quad (3)$$

3.2. Branching behavior of existing formulations

As observed by Vielma et al. (2010) and in our computational experiments, logarithmic formulations such as LogE can offer a considerable computational advantage over other approaches, particularly for univariate piecewise linear functions with many segments (i.e. large d). However, it has also been observed that variable branching with logarithmic formulations such as LogE can produce weak dual bounds (e.g. Martin et al. (2006), Rebennack (2016), Yildiz and Vielma (2013)).

To quantitatively assess relaxation strength after branching, we consider two metrics. The first is the volume of the projection of the LP relaxation onto (x, z) -space (cf. (Lee et al. 2018) for a recent work using volume as a metric for formulation quality). The second is the proportion of the function domain where the LP relaxation after branching is stronger than the LP relaxation before

branching. More formally, if D is the domain of f , F is the projection of the original LP relaxation onto (x, z) -space, and F' is the same projection of the LP relaxation after branching, then we report $\frac{1}{\text{Vol}(D)} \text{Vol}(\{x \in D \mid \min_{(x,z) \in F} z < \min_{(x,z) \in F'} z\})$, which we dub the *strengthened proportion*.

We turn to the LogE formulation for $d = 4$ given in Example 3. The mapping from the λ variables to the original space is $(x, z) = (0, 0)\lambda_1 + (1, 4)\lambda_2 + (2, 7)\lambda_3 + (3, 9)\lambda_4 + (4, 10)\lambda_5$. Qualitatively, in the top row of Figure 2 we see that the LP relaxation, projected onto the (x, z) -space of the graph $\mathbf{gr}(f)$, remains largely unchanged in the down-branching subproblem (i.e. when we branch $y_1 \leq 0$). This is undesirable, as it will not improve dual bounds in a branch-and-bound setting, which is crucial to ensuring fast convergence. Quantitatively, the strengthened proportion for this down-branch is 0, and so when minimizing f , the dual bound will be the same after branching as for the original LP relaxation (assuming both are feasible). From this, it is reasonable to infer that the high-performance of the LogE formulation is due to its strength and small size, and in spite of its poor branching behavior.

In contrast, the traditional SOS2 constraint branching (Beale and Tomlin 1970) induces much more balanced branches in (x, z) -space. Additionally, the incremental Inc formulation (Dantzig 1960, Padberg 2000, Croxton et al. 2003) is a MIP formulation that induces the same branching behavior, which we depict in the bottom row of Figure 2. Quantitatively, both up- and down-branching result in subproblems with a strengthened proportion of 1, meaning that the formulation will always lead to strictly stronger dual bounds when minimizing f . In particular, we highlight the *incremental branching* behavior of the Inc formulation in the (x, z) -space: after selecting for branching a binary variable y_k (Inc has $d - 1$ binary variables, so $k \in \llbracket d - 1 \rrbracket$), the only points $(x, z) \in \mathbf{gr}(f)$ feasible for the down-branch (resp. up-branch) are those that lie on segments 1 to $k - 1$, $\bigcup_{i=1}^{k-1} S^i$ (resp. k to d , $\bigcup_{i=k}^d S^i$). Additionally, the Inc formulation is *hereditarily sharp*: each subproblem LP relaxation projects to exactly the convex hull (either $\text{Conv}(\bigcup_{i=1}^{k-1} S^i)$ or $\text{Conv}(\bigcup_{i=k}^d S^i)$) of the segments feasible for that subproblem (Jeroslow and Lowe 1984, Jeroslow 1988). This combination has been observed to lead to very balanced branch-and-bound trees (Yildiz and Vielma 2013, Vielma 2015), and the Inc formulation has been observed to perform very well for small d , before its size (which scales linearly in d) becomes overwhelming (see the computational results in Section 3.4).

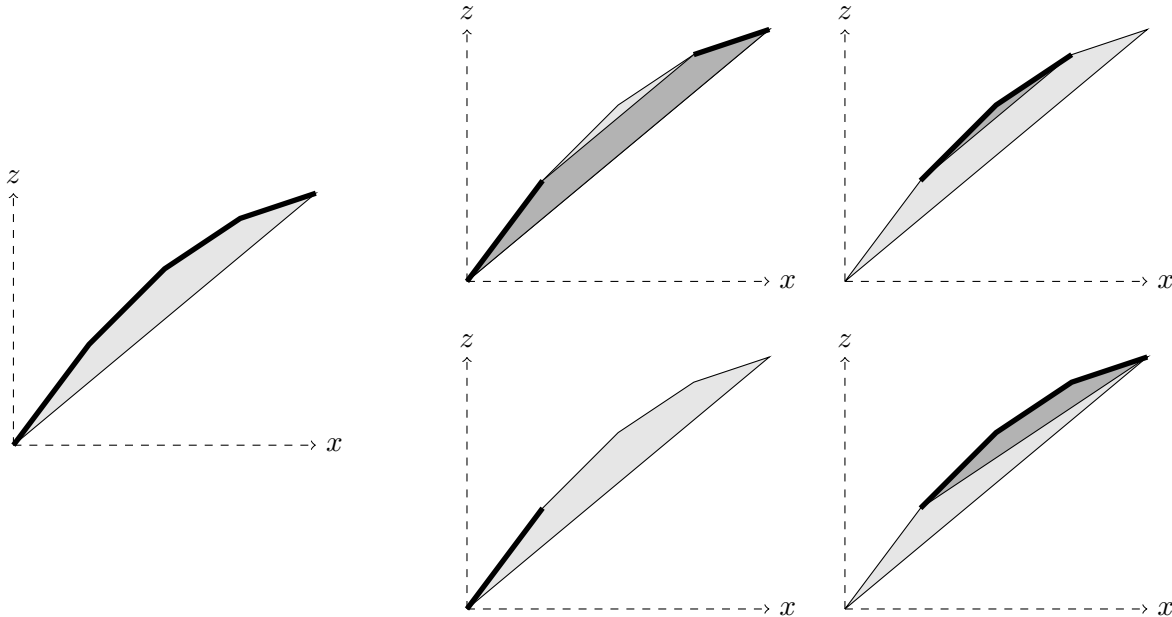


Figure 2 (Left) The LP relaxation of an ideal formulation (e.g. LogE) (3)

projected onto (x, z) -space. The LogE formulation after **(top center)** down-branching $y_1 \leq 0$ and **(top right)** up-branching $y_1 \geq 1$. The Inc formulation after **(bottom center)** down-branching $y_1 \leq 0$ and **(bottom right)** up-branching $y_1 \geq 1$.

3.3. New zig-zag formulations for the SOS2 constraint

We now present new embedding formulations for the SOS2 constraint that retain the size and strength of the LogE formulation, while repairing its degenerate branching behavior. For the remainder of the subsection, assume without loss of generality (w.l.o.g.) that d is a power-of-two. Otherwise, construct the formulation for $\bar{d} = 2^{\lceil \log_2(d) \rceil}$ and fix the extraneous λ_v variables to zero.

Take $K^r \in \mathcal{H}_r(d)$ as the BRGC for $d = 2^r$ elements. Our first new encoding is the transformation of $K^r \in \{0, 1\}^{d \times n}$ to $C^r \in \mathbb{Z}^{d \times r}$, where $C_{i,k}^r = \sum_{j=2}^i |K_{j,k}^r - K_{j-1,k}^r|$ for each $i \in \llbracket d \rrbracket$ and $k \in \llbracket r \rrbracket$. In words, $C_{i,k}^r$ is the number of times the sequence $(K_{1,k}^r, \dots, K_{i,k}^r)$ changes value, and is monotonic nondecreasing in i . Our second encoding will be $Z^r \in \{0, 1\}^{d \times r}$ with $Z_i^r = \mathcal{A}(C_i^r)$ for each $i \in \llbracket d \rrbracket$, where $\mathcal{A} : \mathbb{R}^r \rightarrow \mathbb{R}^r$ is the linear map given by $\mathcal{A}(y)_k = y_k - \sum_{\ell=k+1}^r y_\ell$ for each component $k \in \llbracket r \rrbracket$. We show the encodings for $r = 3$ in Figure 3, and include formal recursive definitions for them in Appendix A, where we additionally show that $C^r, Z^r \in \mathcal{H}_r(d)$. Applying Proposition 2 with the new encodings gives two new small, strong formulations for the SOS2 constraint.

PROPOSITION 3. Take $r = \lceil \log_2(d) \rceil$, along with $C_0^r \equiv C_1^r$ and $C_{d+1}^r \equiv C_d^r$ for notational simplicity. Then two ideal formulations for the SOS2 constraint with d segments are given by

$$\sum_{v=1}^{d+1} C_{v-1,k}^r \lambda_v \leq y_k \leq \sum_{v=1}^{d+1} C_{v,k}^r \lambda_v \quad \forall k \in \llbracket r \rrbracket, \quad (\lambda, y) \in \Delta^{d+1} \times \mathbb{Z}^r \quad (4)$$

and

$$\sum_{v=1}^{d+1} C_{v-1,k}^r \lambda_v \leq y_k + \sum_{\ell=k+1}^r 2^{\ell-k-1} y_\ell \leq \sum_{v=1}^{d+1} C_{v,k}^r \lambda_v \quad \forall k \in \llbracket r \rrbracket, \quad (\lambda, y) \in \Delta^{d+1} \times \{0, 1\}^r. \quad (5)$$

We dub (5) the *binary zig-zag* (ZB) formulation for the SOS2 constraint, as its associated binary encoding Z^r “zig-zags” through the interior of the unit hypercube (See Figure 3). We will refer to formulation (4) as the *general integer zig-zag* (ZZI) formulation because of its use of general integer encoding $C^r \in \mathbb{Z}^{d \times r}$. We emphasize that ZZI and ZB are logarithmically-sized in d and ideal: the same size and strength as the existing LogE formulation.

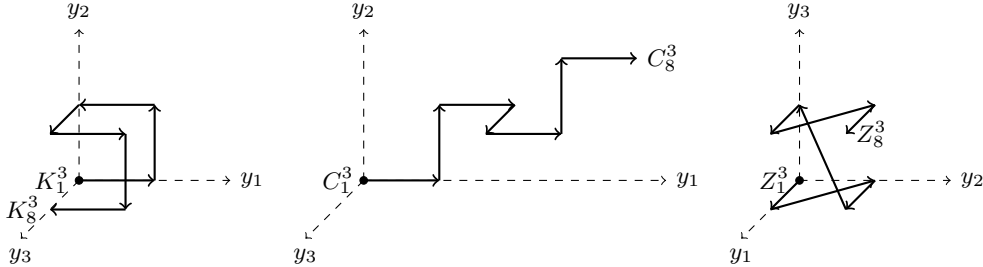


Figure 3 Depiction of K^3 (Left), C^3 (Center), and Z^3 (Right). The first row of each is marked with a dot, and the subsequent rows follow along the arrows. The axis orientation is different for Z^3 for visual clarity.

To study the branching behavior of the ZZI formulation, we return to the SOS2 constraint with $d = 4$ from Example 3. The formulation consists of all $(\lambda, y) \in \Delta^5 \times \mathbb{Z}^2$ such that

$$\lambda_3 + \lambda_4 + 2\lambda_5 \leq y_1 \leq \lambda_2 + \lambda_3 + 2\lambda_4 + 2\lambda_5, \quad \lambda_4 + \lambda_5 \leq y_2 \leq \lambda_3 + \lambda_4 + \lambda_5. \quad (6)$$

We have two possibilities for branching on y_1 , depicted in Figure 4: down on $y_1 \leq 0$ and up on $y_1 \geq 1$, or down on $y_1 \leq 1$ and up on $y_1 \geq 2$. We note that after imposing either $y_1 \leq 0$ or $y_1 \geq 2$, the relaxation is then exact, i.e. the relaxation is equal to exactly one of the segments of the graph

of f . Furthermore, when imposing either $y_1 \leq 1$ or $y_1 \geq 1$, we deduce a general inequality on the λ variables that improves the strengthened proportion relative to LogE: either $\lambda_1 \leq \lambda_4 + \lambda_5$ or $\lambda_5 \leq \lambda_1 + \lambda_2$, respectively.

Statistic	LP Relaxation	LogE 0 ↓	LogE 1 ↑	Inc 0 ↓	Inc 1 ↑	ZZI 0 ↓	ZZI 1 ↑	ZZI 1 ↓	ZZI 2 ↑
Volume	6	5.5	0.5	0	2	0	3.5	3.5	0
Strengthened Prop.	0	0	1	1	1	1	0.5	0.5	1

Table 2 Metrics for each possible branching decision on z_1 for LogE, Inc, and ZZI applied to (1).

As we see qualitatively in Figures 2 and 4 and quantitatively in Table 2, the ZZI formulation yields LP relaxations after branching that are stronger and more balanced than those of the LogE formulation. In Appendix C, we offer a more complex example with an 8-segment concave piecewise linear function where this effect is even more pronounced. An instructive way to interpret the branching of ZZI is that it emulates the SOS2 branching induced by the Inc formulation. In particular, the ZZI formulation also induces incremental branching, but has slightly weaker subproblem relaxations compared to the Inc formulation as it does not maintain the hereditary sharpness property. In this way, the ZZI formulation maintains the size and strength of the LogE formulation, while inducing branching behavior that is much closer to the Inc formulation.

3.4. Univariate computational experiments

To evaluate the new ZZI and ZZB formulations against the existing formulations for univariate piecewise linear functions, we reproduce a variant of the computational experiments of Vielma et al. (2010), with the addition of the ZZB and ZZI formulations. Although the LogIB formulation outperformed the rest of the formulations considered in Vielma et al. (2010), it has also been observed that logarithmic formulations tends to suffer from a significant performance degradation when the number of segments d of the piecewise linear functions is not a power-of-two (Vielma and Nemhauser 2011, Coppersmith and Lee 2005, Muldoon 2012, Muldoon et al. 2013). Therefore, we will focus on problems of this form in our computational experiments. This is precisely the setting in which LogE and LogIB (which we will introduce more formally in Section 4.1) are not equivalent, and

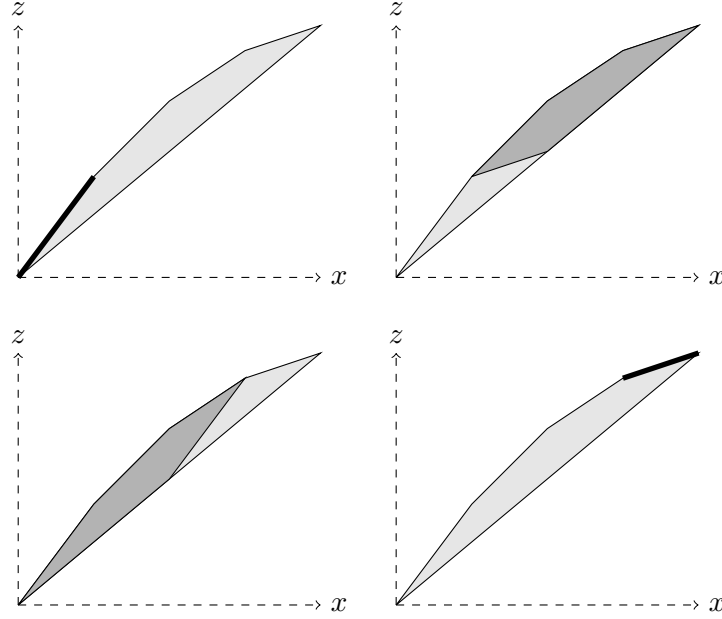


Figure 4 The LP relaxation of the ZZI formulation (6) projected onto (x, z) -space, after down-branching $y_1 \leq 0$ (**top center**), up-branching $y_1 \geq 1$ (**bottom center**), down-branching $y_1 \leq 1$ (**top right**), and up-branching $y_1 \geq 2$ (**bottom right**).

so we include both variants in our experiments. Finally, we also include the previously mentioned Inc formulation, the MC, CC, and DLog formulations as described by Vielma et al. (2010), as well as the SOS2 native branching (SOS2) implementation of the corresponding MIP solver.

We evaluate our formulations on single commodity transportation problems of the form

$$\begin{aligned} \min_{x \geq 0} \quad & \sum_{i \in S} \sum_{j \in D} f_{i,j}(x_{i,j}) \\ \text{s.t.} \quad & \sum_{i \in S} x_{i,j} = d_j \quad \forall j \in D, \quad \sum_{j \in D} x_{i,j} = s_i \quad \forall i \in S, \end{aligned}$$

where we match supply from nodes S with demand from nodes D , while minimizing the transportation costs given by the sum of continuous nondecreasing concave univariate piecewise linear functions $f_{i,j}$ for each arc pair in $S \times D$.

We perform a scaling analysis along two axes: the size of the network (i.e. the cardinality of S and D), and the number of segments for each piecewise linear function $f_{i,j}$. Regarding the first axis, we study both *small* networks ($|S| = |D| = 10$) and *large* networks ($|S| = |D| = 20$). Regarding the

second axis, we study families of instances where each piecewise linear function has $d \in \{6, 13, 28, 59\}$ segments.

We use CPLEX v12.7.0 with the JuMP algebraic modeling library (Dunning et al. 2017) in the Julia programming language (Bezanson et al. 2017) for all computational trials, here and for the remainder of this work. All such trials were performed on an Intel i7-3770 3.40GHz Linux workstation with 32GB of RAM. For each trial, we allow the solver to run for 30 minutes to prove optimality before timing out. For each formulation and each family ($d \in \{6, 13, 28, 59\}$) of 100 instances, we report the average solve time, standard deviation in solve time, and the number of instances for which the formulation was either the fastest (Win), or was unable to prove to optimality in 30 minutes or less (Fail).

We start by studying the small network instances in Table 3. We observe that the Inc formulation is superior for smaller function instances (i.e. with functions with fewer segments). Additionally, the LogE and LogIB formulations have similar performance on all families of instances. We observe that the new ZZI and ZZB formulations are the best performers for larger function instances, and one of the two is the fastest formulation for every instance in the largest function family with $d = 59$. Additionally, ZZI and ZZB both offer roughly a 2x speed-up in average solve time over LogE and LogIB for most families of instances ($d \in \{13, 28, 59\}$).

In Table 4 we present computational results for the large network instances. Here we observe a roughly 2-3x average speed-up on larger function instances for our new formulations over previous methods. Moreover, we highlight that the new formulations have lower variability in solve time, and time out on fewer instances than the existing methods. With $d = 28$, the SOS2 approach works very well for easier instances, winning on 11 of 100, though its variability is extremely high, timing out on 80 of 100 instances. The existing Inc, DLog, LogE, and LogIB formulations all perform roughly comparably.

In Table 5, we focus on those large network problems that are difficult (i.e. no approach is able to solve the instance in under 100 seconds) but still solvable (i.e. one formulation solves the

d	Metric	MC	CC	SOS2	Inc	DLog	LogE	LogIB	ZZB	ZZI
6	Mean (s)	0.6	3.8	1.1	0.6	1.1	1.4	2.6	1.1	0.9
	Std	0.3	4.1	1.5	0.3	1.0	1.2	2.4	0.9	0.5
	Win	35	0	7	46	5	1	0	4	2
	Fail	0	0	0	0	0	0	0	0	0
13	Mean (s)	3.0	71.2	4.5	1.7	4.6	4.4	4.2	2.4	2.6
	Std	3.1	152.0	5.8	0.7	3.5	3.4	3.0	1.8	1.7
	Win	11	0	9	47	11	0	0	15	7
	Fail	0	0	0	0	0	0	0	0	0
28	Mean (s)	18.4	178.9	87.4	5.5	11.1	8.8	8.9	5.1	4.6
	Std	26.0	359.3	309.3	4.4	8.1	5.6	5.4	3.7	2.7
	Win	1	0	6	14	1	0	0	37	41
	Fail	0	3	3	0	0	0	0	0	0
59	Mean (s)	348.7	541.0	664.3	17.1	19.1	16.3	16.0	9.8	9.3
	Std	523.7	610.3	746.4	14.9	11.3	10.3	9.3	6.1	5.0
	Win	0	0	0	0	0	0	0	41	59
	Fail	7	13	26	0	0	0	0	0	0

Table 3 Computational results with CPLEX for univariate transportation problems on small networks.

d	Metric	MC	CC	SOS2	Inc	DLog	LogE	LogIB	ZZB	ZZI
28	Mean (s)	828.0	1769.3	1498.6	196.9	242.1	332.9	295.8	147.4	98.0
	Std	714.3	211.5	646.9	206.8	282.2	430.4	387.9	228.2	144.4
	Win	0	0	11	6	1	1	5	10	66
	Fail	28	97	80	0	1	2	2	1	0
59	Mean (s)	1596.9	1800.0	1800.0	793.4	777.1	749.3	753.5	328.7	273.1
	Std	475.7	-	-	557.7	593.5	593.3	591.3	383.0	341.6
	Win	0	0	0	2	0	1	1	29	67
	Fail	82	100	100	11	15	16	17	2	2

Table 4 Computational results with CPLEX for univariate transportation problems on large networks.

Metric	MC	CC	SOS2	Inc	DLog	LogE	LogIB	ZZB	ZZI
Mean (s)	1663.4	1800.0	1800.0	710.6	752.4	793.1	796.0	319.3	261.4
Std	298.7	-	-	529.9	555.0	570.9	554.4	392.7	316.7
Win	0	0	0	4	0	1	0	27	53
Fail	78	85	85	10	15	17	18	2	1
Margin	-	-	-	207.0	-	5.6	-	320.1	348.9

Table 5 Difficult univariate transportation problems on large networks.

instance in under 30 minutes). We see that the new zig-zag formulations are the fastest on 80 of 85 such instances. We also report the average margin: for those instances for which a given new (resp. existing) formulation is fastest, what is the absolute difference in solve time between it and the fastest existing (resp. new) formulation? In this way, we can measure the absolute improvement offered by our new formulation on an instance-by-instance basis. Here we see that the new formulations offer a substantial improvement on these difficult instances, with an absolute decrease of 5-6 minutes in average solve time over existing methods. Finally, we highlight that there are 5 instances that our new formulations can solve to optimality and for which all existing formulations are unable to solve in 30 minutes.

We repeat the same experiments with the Gurobi v7.0.2 solver depicted in Tables 3 and 4, and include the results in Tables 6 and 7, respectively. On the whole, Gurobi is capable of solving these univariate instances much more efficiently than CPLEX; we omit an analogue of Table 5 as none of the instances satisfy the specified hardness criteria. Gurobi has a relatively superior implementation of native SOS2 branching that works very well for small and medium function instances. However, it performs very poorly on large function instances (timing out on 98 of 100 instances with $d = 59$). We again observe on these larger instances that the ZZI formulation offers a net improvement over the existing host of logarithmic formulations, and is the winner on a plurality of the largest instances in both families. However, as the solve time for all logarithmic formulations on the these largest univariate instances is relatively much lower with Gurobi than CPLEX, the average improvement of the new formulations is more muted than that which can be observed in Tables 4 and 5.

d	Metric	MC	CC	SOS2	Inc	DLog	LogE	LogIB	ZZB	ZZI
6	Mean (s)	0.8	2.7	0.2	0.5	0.7	0.7	0.7	1.0	0.7
	Std	0.4	3.4	0.2	0.2	0.8	0.7	0.8	0.8	0.6
	Win	0	0	95	2	1	1	0	0	1
	Fail	0	0	0	0	0	0	0	0	0
13	Mean (s)	4.2	13.4	0.9	1.9	4.1	5.2	2.1	2.5	2.7
	Std	4.8	15.3	1.0	0.9	4.5	6.0	2.9	2.6	2.3
	Win	0	0	90	4	0	0	1	2	3
	Fail	0	0	0	0	0	0	0	0	0
28	Mean (s)	30.3	95.2	3.9	6.1	9.2	6.1	3.3	4.4	4.4
	Std	43.0	261.3	8.1	5.2	8.7	10.2	2.7	4.6	3.7
	Win	0	0	63	1	1	7	8	7	13
	Fail	0	2	0	0	0	0	0	0	0
59	Mean (s)	265.5	372.3	1781.2	24.3	7.3	12.6	9.1	7.5	6.0
	Std	409.5	530.0	134.7	23.1	6.7	12.5	9.3	7.2	5.3
	Win	0	0	0	0	10	20	16	5	49
	Fail	2	8	98	0	0	0	0	0	0

Table 6 Computational results with Gurobi for univariate transportation problems on small networks.

d	Metric	MC	CC	SOS2	Inc	DLog	LogE	LogIB	ZZB	ZZI
28	Mean (s)	124.6	245.8	1784.8	31.5	27.1	19.8	16.3	19.7	17.0
	Std	192.9	321.4	151.9	16.1	15.8	15.3	6.8	11.3	9.3
	Win	0	0	0	0	5	16	38	11	30
	Fail	0	2	99	0	0	0	0	0	0
59	Mean (s)	619.4	901.2	1800.0	87.3	23.9	27.4	26.3	24.7	20.9
	Std	560.3	683.5	-	53.6	19.7	11.8	14.1	16.5	16.1
	Win	0	0	0	0	10	9	20	7	54
	Fail	12	27	100	0	0	0	0	0	0

Table 7 Computational results with Gurobi for univariate transportation problems on large networks.

4. Formulations for bivariate piecewise linear functions

Bivariate piecewise linear functions possess a much more complex structure than their univariate counterparts, which means that constructing logarithmic formulations for them is also correspondingly more difficult. This combinatorial structure is endowed by the pattern into which the domain is decomposed, the choice of which determines the values which the bivariate piecewise function takes (see Figure 5 for an illustration). Although it is possible to extend the geometric construction of Proposition 2 to the bivariate setting (Huchette and Vielma 2019b), this technique requires us to compute the hyperplanes spanned by high-dimensional vectors a la Proposition 2, which is, in general, very difficult. Instead, we turn to a combinatorial approach.

For the remainder of the section, we will focus on bivariate functions with *grid triangulation* domains, which we define formally as follows.

DEFINITION 2. Presume that $V = \llbracket d_1 + 1 \rrbracket \times \llbracket d_1 + 1 \rrbracket$. A *grid triangulation* \mathcal{T} of V is a family of sets T where:

- Each $T \in \mathcal{T}$ is a triangle: $|T| = 3$.
- \mathcal{T} partitions the domain: $\bigcup_{T \in \mathcal{T}} \text{Conv}(T) = \text{Conv}(V)$ and $\text{relint}(\text{Conv}(T)) \cap \text{relint}(\text{Conv}(T')) = \emptyset$ for each distinct $T, T' \in \mathcal{T}$ (where $\text{relint}(S)$ is the (relative) interior of set S).
- \mathcal{T} is on a regular grid: $\|v - w\|_\infty \leq 1$ for each $T \in \mathcal{T}$ and $v, w \in T$.

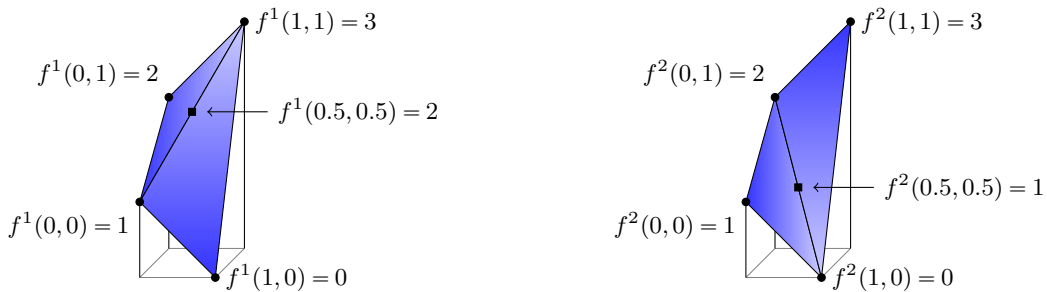


Figure 5 Two bivariate functions over $D = [0, 1]^2$ that match on the gridpoints, but differ on the interior of D .

4.1. Independent branching formulations

The original logarithmic formulation LogIB of Vielma and Nemhauser (2011) for the SOS2 constraint is derived from the class of *independent branching* formulations, which offers a combinatorial way of constructing formulations. Huchette and Vielma (2019a) offer a complete characterization of its expressive power, as well as a graphical procedure to systematically construct independent branching formulations. We start with two definitions.

DEFINITION 3. Take a combinatorial disjunctive constraint given by the family of subsets $(T^i)_{i=1}^d$ over a ground set V .

- The *conflict graph* $G = (V, E)$ of the combinatorial disjunctive constraint is given by the edge set $E = \{ \{u, v\} \in [V]^2 \mid \{u, v\} \not\subseteq T^i \text{ for all } i \in [d] \}$, where $[V]^2 \stackrel{\text{def}}{=} \{ \{u, v\} \in V \times V \mid u \neq v \}$.
- A *biclique* of some graph $G = (V, E)$ is a pair of sets (A, B) such that $(V, A * B)$ is a subgraph of G (i.e. $A * B \subseteq E$), where $A * B \stackrel{\text{def}}{=} \{ \{u, v\} \in [V]^2 \mid u \in A, v \in B \}$.
- A *biclique cover* of some graph $G = (V, E)$ is a family of bicliques $\{(A^k, B^k)\}_{k=1}^r$ such that $E = \bigcup_{k=1}^r (A^k * B^k)$. We say that such a biclique cover has r levels.

Given a biclique cover for the conflict graph of a (suitably representable) combinatorial disjunctive constraint, the technique of Huchette and Vielma (2019a) directly constructs a formulation as follows.

PROPOSITION 4 (Huchette and Vielma (2019a)). Let $\mathcal{T} = (T^i \subseteq V)_{i=1}^d$ be the family of sets corresponding to either a univariate piecewise linear function, or a bivariate piecewise linear function with a grid triangulated domain. Take E as the edge set for the conflict graph corresponding to \mathcal{T} . If $\{(A^k, B^k)\}_{k=1}^r$ is a biclique cover for (V, E) , then an ideal independent branching formulation for $\bigcup_{i=1}^d P(T^i)$ is

$$\sum_{v \in A^k} \lambda_v \leq y_k, \quad \sum_{v \in B^k} \lambda_v \leq 1 - y_k \quad \forall k \in [r], \quad (\lambda, y) \in \Delta^V \times \{0, 1\}^r. \quad (7)$$

Intuitively, this formulation ensures that, for each level k , either $\lambda_v = 0$ for all $v \in A^k$, or $\lambda_v = 0$ for all $v \in B^k$.

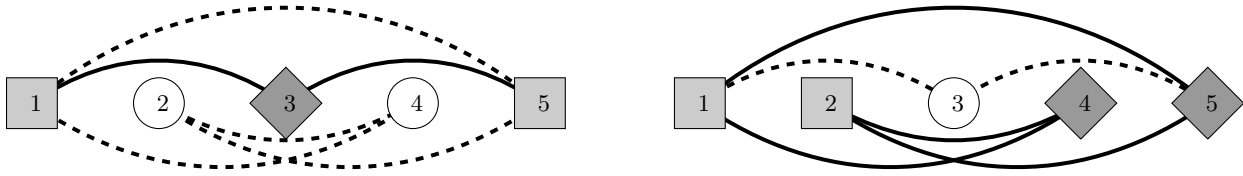


Figure 6 The biclique cover for the conflict graph G of the SOS2 constraint in Example 4. **(Left)** The first level with A^1 and B^1 are diamonds and squares, respectively; and **(Right)** similarly for A^2 and B^2 in the second level. For each level, covered edges are solid and omitted edges are dashed.

As motivation, we return to Example 2 to construct the logarithmic independent branching formulation for the SOS2 constraint, LogIB, as introduced by Vielma and Nemhauser (2011).

EXAMPLE 4. Take the SOS2 constraint with $d = 4$ (as seen in (1)). The edge set for the conflict graph is $E = \{\{1, 3\}, \{1, 4\}, \{1, 5\}, \{2, 4\}, \{2, 5\}, \{3, 5\}\}$, which admits a biclique cover with the sets $A^1 = \{3\}$, $B^1 = \{1, 5\}$, $A^2 = \{4, 5\}$, and $B^2 = \{1, 2\}$. The corresponding LogIB formulation is then

$$\lambda_3 \leq y_1, \quad \lambda_1 + \lambda_5 \leq 1 - y_1, \quad \lambda_4 + \lambda_5 \leq y_2, \quad \lambda_1 + \lambda_2 \leq 1 - y_2, \quad (\lambda, y) \in \Delta^V \times \{0, 1\}^2. \quad (8)$$

See Figure 6 for an illustration. As noted previously, the LogIB formulation (8) coincides with the LogE formulation (3) because d is a power-of-two; see Appendix B for an instance where this is not the case.

4.2. Independent branching formulations for bivariate piecewise linear functions

Recall that, using Proposition 4, we can immediately construct a formulation for a bivariate function that is ideal and of size $\mathcal{O}(r)$ if we can find a biclique cover with r levels for the corresponding conflict graph. A natural question then is: what is the smallest biclique cover that be constructed for a given grid triangulation?

Computing a minimum cardinality biclique cover is NP-hard, even on bipartite graphs (Garey and Johnson 1979).² Vielma and Nemhauser (2011) consider a highly structured grid triangulation known as the J1 or Union Jack (Todd 1977), and (implicitly) present a biclique cover with $r = \lceil \log_2(d_1) \rceil + \lceil \log_2(d_2) \rceil + 1$ levels. More recently, Huchette and Vielma (2019a) propose a construction

under a weaker structural condition involving the existence of a certain graph coloring that uses at most $r = \lceil \log_2(d_1) \rceil + \lceil \log_2(d_2) \rceil + 2$ levels, as well as a construction for arbitrary grid triangulations with $r = \lceil \log_2(d_1) \rceil + \lceil \log_2(d_2) \rceil + 9$ levels. In this work, we present a new, even smaller construction that is applicable for any grid triangulation.

For the remainder of the subsection, consider a family of sets \mathcal{T} associated with a grid triangulation with $V = \llbracket d_1 + 1 \rrbracket \times \llbracket d_2 + 1 \rrbracket$, along with the edge set E for its corresponding conflict graph. It will be useful to decompose these edges into three classes:

$$\begin{aligned}
 E^{\nearrow} &\stackrel{\text{def}}{=} \{ \{u, v\} \in E \mid \|u - v\|_\infty = 1, |(u_1 - v_1) + (u_2 - v_2)| = 2 \} \\
 E^{\searrow} &\stackrel{\text{def}}{=} \{ \{u, v\} \in E \mid \|u - v\|_\infty = 1, |(u_1 - v_1) + (u_2 - v_2)| = 0 \} \\
 E^F &\stackrel{\text{def}}{=} \{ \{u, v\} \in E \mid \|u - v\|_\infty > 1 \}.
 \end{aligned}$$

In words, E^{\nearrow} and E^{\searrow} are those “nearby” edges sharing a common subrectangle that are oriented along a diagonal (southwest to northeast) or an anti-diagonal (southeast to northwest), respectively. Contrastingly, E^F are those edges that are “far apart.” It is straightforward from their definition to see that the three classes form a partition of E .

First, we show how to exactly cover the “far apart” edges by applying an aggregated SOS2 construction along each axis.

LEMMA 1. *Take $\{(A^{1,k}, B^{1,k})\}_{k=1}^{r_1}$ and $\{(A^{2,k}, B^{2,k})\}_{k=1}^{r_2}$ as biclique covers for the conflict graphs associated with the SOS2 constraints on $d_1 + 1$ and $d_2 + 1$ breakpoints, respectively. Then*

$$E^F = \bigcup_{k=1}^{r_1} ((A^{1,k} \times \llbracket d_2 + 1 \rrbracket) * (B^{1,k} \times \llbracket d_2 + 1 \rrbracket)) \cup \bigcup_{k=1}^{r_2} ((\llbracket d_1 + 1 \rrbracket \times A^{2,k}) * (\llbracket d_1 + 1 \rrbracket \times B^{2,k})). \quad (9)$$

Proof The conflict graph for the SOS2 constraint on $d + 1$ breakpoints is given by the edge set $\{ \{u, v\} \in [d + 1]^2 \mid |u - v| > 1 \}$. Therefore, if the families of sets are taken as described, we can infer that

$$\{ \{u, v\} \in [V]^2 \mid |u_1 - v_1| > 1 \} = \bigcup_{k=1}^{r_1} ((A^{1,k} \times \llbracket d_2 + 1 \rrbracket) * (B^{1,k} \times \llbracket d_2 + 1 \rrbracket)) \quad (10a)$$

$$\{ \{u, v\} \in [V]^2 \mid |u_2 - v_2| > 1 \} = \bigcup_{k=1}^{r_2} ((\llbracket d_1 + 1 \rrbracket \times A^{2,k}) * (\llbracket d_1 + 1 \rrbracket \times B^{2,k})). \quad (10b)$$

Observe that the union of the left-hand sides of both equations in (10) is equal to E^F , while the union of the right-hand sides of both equations in (10) is identical to the right-hand side of (9), giving the result. \square

Next, we introduce an algorithm that constructs three bicliques. Each “nearby” edge in the conflict graph that is oriented along a diagonal will be contained in one of these 3 bicliques. However, these 3 bicliques also introduce additional edges that are not “nearby” edges oriented along a diagonal, and so the bicliques do not induce subgraphs of the graph induced by the diagonal edges, (V, E^\nearrow) . Fortunately, we will show that these extra edges are “far apart” edges contained in E^F , and so the 3 bicliques *do* induce subgraphs of the conflict graph (V, E) as required by Proposition 4. Therefore, we can use these bicliques to construct a cover for the conflict graph; they will cover each “nearby” edge oriented along a diagonal, while not introducing any undesired additional “nearby” edges.

LEMMA 2. *For each $\tau \in \{0, 1, 2\}$, construct the sets $(A^\tau, B^\tau) = \text{DIAGONALBICLIQUES}(\tau, E^\nearrow)$ according to the procedure listed in Algorithm 1. Then $E^\nearrow \subseteq \bigcup_{\tau=0}^2 (A^\tau * B^\tau) \subseteq E$.*

Proof The first inclusion: $E^\nearrow \subseteq \bigcup_{\tau=0}^2 (A^\tau * B^\tau)$ Consider some arbitrary $(i, j) \in \llbracket d_1 \rrbracket \times \llbracket d_2 \rrbracket$. It suffices to show that there exists some value for $\tau \in \{0, 1, 2\}$ and some κ such that either: a) $\kappa \in \{\tau, \tau + 3, \dots, d_1 - 1\}$ and $j = i - \kappa$, or b) $\kappa \in \{3 - \tau, 6 - \tau, \dots, d_2 - 1\}$ and $i = j - \kappa$. If this is the case, then Algorithm 1 will reach either line 6 or 16, respectively, with the appropriate values for (i, j) , and so if $\{(i, j), (i + 1, j + 1)\} \in E^\nearrow$, by construction we will have build (A, B) such that $\{(i, j), (i + 1, j + 1)\} \in A * B$.

To show that such a values exists, first consider the case where $i > j$, in which case $i - j \in \{0, \dots, d_1 - 1\}$. It is straightforward to see that, if we take $\tau = (i - j) \bmod 3$, then $\tau \in \{0, 1, 2\}$, and moreover one of the iterations of the for loop initiated in line 2 will have $\kappa = i - j$, giving the desired result. Similarly, if $i < j$, we can attain any value $\kappa \in \{1, \dots, d_2 - 1\}$ in the loop initiated in line 12; choose $\kappa = j - i$ to give the result. Therefore, we conclude that $E^\nearrow \subseteq \bigcup_{\tau=0}^2 (A^\tau * B^\tau)$.

To second inclusion: $\bigcup_{\tau=0}^2 (A^\tau * B^\tau) \subseteq E$ We start by observing that, due to the for loop ranges and the explicit checks on the values of j and i in lines 6 and 16, respectively, any pair $\{u =$

Algorithm 1 Computing bicliques that cover diagonal triangle selection edges.

Require: Integer $\tau \in \{0, 1, 2\}$.

```

1: procedure DIAGONALBICLIQUES( $\tau, E$ )
2:   for  $\kappa \leftarrow \tau, \tau + 3, \dots, d_1 - 1$  do
3:      $\phi \leftarrow \text{true}$ 
4:     for  $i \leftarrow (1 + \kappa), \dots, d_1$  do
5:        $j \leftarrow i - \kappa$ 
6:       if  $1 \leq j \leq d_2$  and  $\{(i, j), (i + 1, j + 1)\} \in E$  then
7:         if  $\phi$  then
8:           Insert  $(i, j) \rightarrow A$  and  $(i + 1, j + 1) \rightarrow B$ 
9:         else
10:          Insert  $(i + 1, j + 1) \rightarrow A$  and  $(i, j) \rightarrow B$ 
11:           $\phi \leftarrow \neg\phi$             $\triangleright$  The unary operator  $\neg$  denotes the negation of a boolean
12:       for  $\kappa \leftarrow 3 - \tau, 6 - \tau, \dots, d_2 - 1$  do
13:          $\phi \leftarrow \text{true}$ 
14:         for  $j \leftarrow (1 + \kappa), \dots, d_2$  do
15:            $i \leftarrow j - \kappa$ 
16:           if  $1 \leq i \leq d_1$  and  $\{(i, j), (i + 1, j + 1)\} \in E$  then
17:             if  $\phi$  then
18:               Insert  $(i, j) \rightarrow A$  and  $(i + 1, j + 1) \rightarrow B$ 
19:             else
20:               Insert  $(i + 1, j + 1) \rightarrow A$  and  $(i, j) \rightarrow B$ 
21:                $\phi \leftarrow \neg\phi$ 
22:       return  $(A, B)$ 

```

$(i, j), v = (i + 1, j + 1)\}$ that could possibly be inserted into (A, B) at lines 8, 10, 18, or 20 will naturally satisfy $u, v \in V \equiv \llbracket d_1 + 1 \rrbracket \times \llbracket d_2 + 1 \rrbracket$.

Next, observe that by the definition of a grid triangulation, for each $u, v \in V$ with $\|u - v\|_\infty > 1$, necessarily $\{u, v\} \in E^F \subseteq E$. Therefore, the result follows if we can show that, for each $\tau \in \{0, 1, 2\}$, any $\{u, v\} \in (A^\tau * B^\tau) \setminus E^\nearrow$ satisfies $\|u - v\|_\infty > 1$, and therefore $\{u, v\} \in E^F$.

For the remainder of the proof fix $\tau \in \{0, 1, 2\}$ and presume some element $u = (i + \Delta, j + \Delta)$ was inserted into set A on line 8 ($\Delta = 0$) or on line 10 ($\Delta = 1$) with the iteration value κ for the loop initiated on line 2. We will inspect possible values $v = (i' + \Delta', j' + \Delta')$ that can be inserted into set B at lines 8 or 18 ($\Delta' = 1$), or lines 10 or 20 ($\Delta' = 0$) to verify that $\{u, v\} \in E^F$. All other possible cases will follow by symmetry.

First, consider possible insertions of v to set B on line 8 or 10 with the same iteration value κ in the for loop initiated on line 2. Presume that $i' \neq i$ are distinct iteration values for the loop initiated on line 4. Take ϕ and ϕ' as the values for the boolean for each loop iteration, and presume w.l.o.g. that $\phi = \text{true}$ (and, therefore, that $\Delta = 0$). If $i' = i + 1$, then due to the negation on line 11, $\phi' = \text{false}$. Therefore, the two passes through the loop introduce exactly the elements $(i, j), (i + 2, j + 2) \rightarrow A$ and $(i + 1, j + 1) \rightarrow B$, and so no unnecessary edges are introduced. An analogous argument holds if $i' = i - 1$. If, on the other hand, $|i - i'| > 1$, presume w.l.o.g. that $i' > i$, and observe that the elements added to the sets in the two loop iterations are $(i, j), (i' + \Delta', j' + \Delta') \rightarrow A$ and $(i + 1, j + 1), (i' + 1 - \Delta', j' + 1 - \Delta') \rightarrow B$, where $\Delta' = 0$ if $\phi' = \text{true}$ and $\Delta' = 1$ otherwise. Then $|i - (i' + 1 - \Delta')| = |(i' - i) + (1 - \Delta')| > 1$, and so $\{(i, j), (i' + \Delta')\} \in E^F$. A similar argument holds for the other edges introduced, and for the case where $\phi = \text{false}$, and so, restricted to this single pass through the for loop, we have the result.

Next, consider possible insertions of v to set B with some distinct iteration value $\kappa' \neq \kappa$ in the for loop initiated on line 2. Since τ is fixed, we have that $|\kappa - \kappa'| \geq 3$. If $|(i + \Delta) - (i' + \Delta')| > 1$, we are done, so presume otherwise. In this case, since $|(i + \Delta) - (i' + \Delta')| \leq 1$ and $|\kappa - \kappa'| \geq 3$, we conclude that

$$|(j + \Delta) - (j' + \Delta')| = |(i + \Delta - \kappa) - (i' + \Delta' - \kappa')|$$

$$\begin{aligned}
&= |((i + \Delta) - (i' + \Delta')) - (\kappa - \kappa')| \\
&\geq |(i + \Delta) - (i' + \Delta')| - |\kappa - \kappa'| \\
&\geq |1 - 3| = 2.
\end{aligned}$$

Therefore, $\{u, v\} \in E^F$.

Finally, consider the case where v was inserted into set B in the for loop initiated on line 12. Define the quantity $\gamma = (i + \Delta) - (j' + \Delta')$. Using the identities $j = i - \kappa$ and $i' = j' - \kappa'$ given by lines 5 and 15, respectively, we can write

$$|(i + \Delta) - (i' + \Delta')| = |(i + \Delta) - (j' + \Delta' - \kappa')| = |\gamma + \kappa'| \quad (11a)$$

$$|(j + \Delta) - (j' + \Delta')| = |(i + \Delta - \kappa) - (j' + \Delta')| = |\gamma - \kappa| \quad (11b)$$

Therefore, in order for $|(i + \Delta) - (i' + \Delta')| \leq 1$ (*condition 1*), we must have $\gamma + \kappa' \in \{-1, 0, 1\}$, i.e. $\gamma \in \{-\kappa' - 1, -\kappa', -\kappa' + 1\}$. Since $\kappa' \geq 3 - \tau$ from the loop iteration definition of line 12, we can then infer that $\gamma \leq \tau - 2$ if this condition holds. Similarly, in order for $|(j + \Delta) - (j' + \Delta')| \leq 1$ (*condition 2*), we must have $\gamma - \kappa \in \{-1, 0, 1\}$, i.e. $\gamma \in \{\kappa - 1, \kappa, \kappa + 1\}$. Since $\kappa \geq \tau$ from the loop iteration definition of line 2, we can infer that $\gamma \geq \tau - 1$ for this condition to hold. As there does not exist a value of γ such that $\gamma \leq \tau - 2$ and $\gamma \geq \tau - 1$, we can infer that both condition 1 and condition 2 cannot hold at the same time. Equivalently, either $|u_1 - v_1| > 1$ or $|u_2 - v_2| > 1$, which implies that $\|u - v\|_\infty > 1$. Therefore, $\{u, v\} \in E^F$, completing the proof. \square

It is straightforward to adapt the construction from Lemma 2 to separate the nearby edges E^\searrow along the anti-diagonals, by, for example, reflecting the ground set V along x_1 direction via the invertible mapping $M : V \rightarrow V$ where $M(u, v) = (d_1 + 2 - u, v)$, and then applying Algorithm 1 to the edge set transformed using this mapping. Additionally, in Appendix D we give an explicit statement from first principles.

LEMMA 3. *There exists a family of bicliques $\{(A^k, B^k)\}_{k=0}^2$ such that $E^\searrow \subseteq \bigcup_{\tau=0}^2 (A^\tau * B^\tau) \subseteq E$.*

Combining these results gives an explicit procedure to construct a small formulation for arbitrary bivariate grid triangulations.

THEOREM 1. *There exists an independent branching formulation for a bivariate grid triangulation over $V = \llbracket d_1 + 1 \rrbracket \times \llbracket d_2 + 1 \rrbracket$ of depth $\lceil \log_2(d_1) \rceil + \lceil \log_2(d_2) \rceil + 6$.*

Proof The construction follows by applying Proposition 4 to the biclique cover given by the union of all pairs of sets as defined in Lemmas 1, 2, and 3. The constructions from Lemmas 2 and 3 each introduce 3 bicliques. Furthermore, as noted in Section 3, Vielma and Nemhauser (2011) presented an independent branching formulation for SOS2 on $d + 1$ breakpoints that requires $\lceil \log_2(d) \rceil$ level, meaning that we can adopt the construction of Lemma 1 using $\lceil \log_2(d_1) \rceil + \lceil \log_2(d_2) \rceil$ bicliques, giving the result. \square

We can show the construction pictorially in Figures 7 and 8 on one particular grid triangulation with $d_1 = d_2 = 8$. In Figure 7, we see the bicliques derived in Lemma 1, where a logarithmically-sized SOS2 biclique is “aggregated” vertically or horizontally (top and bottom rows, respectively). In the top row of Figure 8, we see the construction derived in Lemma 2, which covers all diagonal edges E^\nearrow . Note the three panels, each of which aggregates diagonal lines that are sufficiently far apart, starting with an offset of $\tau \in \{0, 1, 2\}$ (from left to right). In particular, note that all of the edges introduced that are not in E^\nearrow are sufficiently far apart that they are contained in E^F , meaning that no undesired edges are introduced. In the second row of Figure 8, we see the analogous construction that covers the antidiagonal lines presented in Lemma 3.

4.3. Combination of formulations

Since our formulations for bivariate piecewise linear functions are comprised of two (aggregated) SOS2 constraints and a biclique cover for the “triangle selection”, we could potentially replace the independent branching formulations for the two SOS2 constraints with *any* SOS2 formulation and maintain validity. For example, we can construct a *hybrid* formulation for bivariate functions over a grid triangulation by applying the ZZI formulation for the aggregated SOS2 constraint along the x_1 and the x_2 dimension, and the 6-stencil independent branching formulation to enforce triangle selection. However, in general the intersection of ideal formulations will not be ideal,

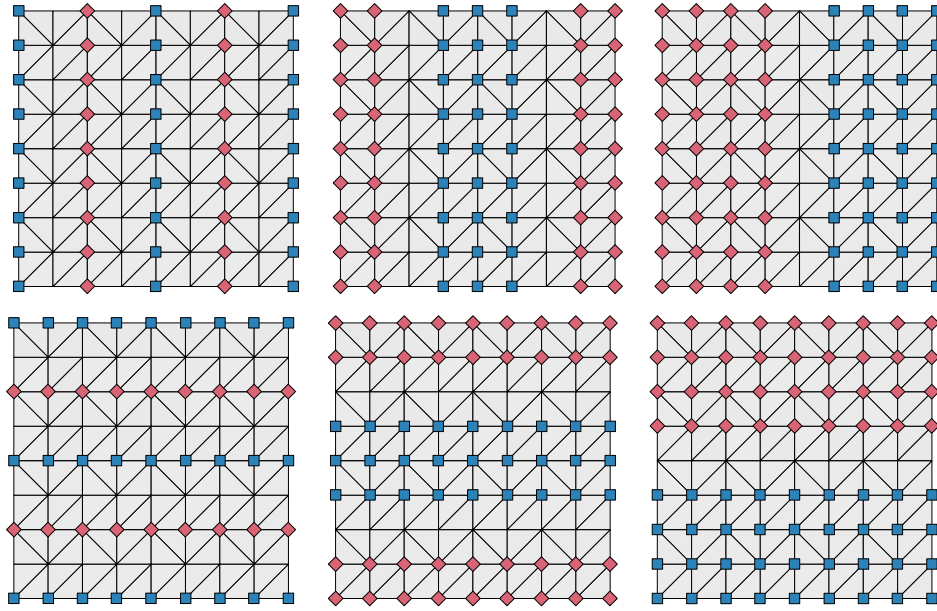


Figure 7 The “aggregated SOS2” biclique construction from Lemma 1. The first row depicts the sets $A^{1,k} \times \llbracket d_2 + 1 \rrbracket$ and $B^{1,k} \times \llbracket d_2 + 1 \rrbracket$ as squares and diamonds, respectively, while the second row depicts the sets $\llbracket d_1 + 1 \rrbracket \times A^{2,k}$ and $\llbracket d_1 + 1 \rrbracket \times B^{2,k}$ as squares and diamonds, respectively.

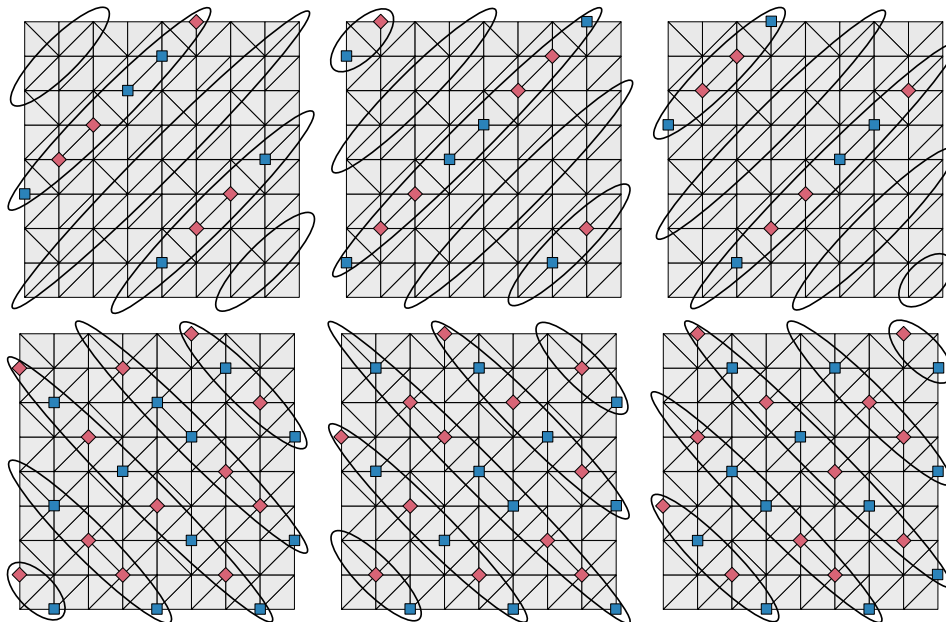


Figure 8 The diagonal and anti-diagonal biclique construction from Lemmas 2 and 3, respectively in the top and bottom rows. In each row, the sets A^τ and B^τ are depicted in squares and diamonds, respectively. As a visual aid, the diagonal/anti-diagonal lines which are covered in each cell are circled.

with independent branching formulations being a notable exception. Fortunately, the following proposition (proven in Appendix E) shows that this preservation of strength is not restricted to independent branching formulations, but holds for any intersection of ideal formulations of combinatorial disjunctive constraints.

THEOREM 2. *Fix $m \in \mathbb{N}$ and take:*

- $U^t = \bigcup_{i=1}^{s_t} P(T^{i,t})$, where $\bigcup_{i=1}^{s_t} T^{i,t} = V$, and
- $\Pi^t \subseteq \mathbb{R}^V \times \mathbb{R}^{r_t}$ such that $\{(\lambda, z^t) \in \Pi^t \mid z^t \in \mathbb{Z}^{r_t}\}$ is an ideal formulation of U^t

for each $t \in \llbracket m \rrbracket$. Then, an ideal formulation for $\bigcap_{t=1}^m U^t$ is

$$\left\{ (\lambda, z^1, \dots, z^m) \left| \begin{array}{l} (\lambda, z^t) \in \Pi^t \quad \forall t \in \llbracket m \rrbracket \\ z^t \in \mathbb{Z}^{r_t} \quad \forall t \in \llbracket m \rrbracket \end{array} \right. \right\}. \quad (12)$$

4.4. Computational experiments with bivariate piecewise linear functions

To study the computational efficacy of the 6-stencil approach, we perform a computational study on a series of bicommodity transportation problems studied in Section 5.2 of Vielma et al. (2010). The network for each instance is fixed with 5 supply nodes and 5 demand nodes, and the objective functions are the sum of 25 concave, nondecreasing bivariate piecewise linear functions over grid triangulations with $d_1 = d_2 = N$ for $N \in \{4, 8, 16, 32\}$. The triangulation of each bivariate function is generated randomly, which is the only difference from (Vielma et al. 2010), where the Union Jack triangulation was used. To handle generic triangulations, we apply the 6-stencil formulation for triangle selection, coupled with either the LogE, ZZB, or ZZI formulation for the SOS2 constraints, taking advantage of Theorem 2 (recall that LogE and LogIB coincide when d is a power-of-two). We compare these new formulations against the CC, MC, and DLog formulations, which readily generalize to bivariate functions. We note in passing that the Inc formulation approach also generalizes to bivariate piecewise linear functions, but requires the computation of a Hamiltonian cycle (Wilson 1998), a nontrivial task which may not be practically viable for unstructured triangulations.

In Table 8, we see that the new formulations are the fastest on every instance in our test bed. For $N \in \{16, 32\}$, we see an average speed-up of over an order of magnitude as compared to the

N	Metric	6-Stencil +					
		MC	CC	DLog	LogE	ZZB	ZZI
4	Mean (s)	1.4	1.5	0.9	0.4	0.4	0.4
	Std	1.3	1.5	0.6	0.2	0.2	0.2
	Win	0	0	0	29	31	40
	Fail	0	0	0	0	0	0
8	Mean (s)	39.3	97.2	12.6	2.7	3.0	3.0
	Std	75.0	179.6	9.8	2.2	2.4	2.9
	Win	0	0	0	51	17	32
	Fail	0	0	0	0	0	0
16	Mean (s)	1370.9	1648.1	352.8	24.6	26.5	35.2
	Std	670.4	360.8	499.4	24.5	27.4	40.4
	Win	0	0	0	43	31	6
	Fail	53	66	6	0	0	0
32	Mean (s)	1800.0	1800.0	1499.6	133.5	167.6	246.5
	Std	-	-	475.2	162.7	226.7	306.6
	Win	0	0	0	63	15	2
	Fail	80	80	50	0	0	1

Table 8 Computational results with CPLEX for bivariate transportation problems on grids of size $N = d_1 = d_2$.

DLog formulation, the best of the existing approaches from the literature. We see that the LogE 6-stencil formulation wins a plurality or majority of instances for $N \in \{8, 16, 32\}$, and that the hybrid ZZI 6-stencil formulation is outperformed by the hybrid ZZB 6-stencil formulation by a non-trivial amount on larger instances. In particular, we highlight the largest family of instances ($N = 32$), where existing methods are unable to solve 50 of 80 instances in 30 minutes or less, whereas our new formulations can solve all in a matter of minutes, on average.

For completeness, we also perform bivariate computational experiments where N is not a power-of-two, now adding the LogIB 6-stencil formulation as an option for the SOS2 constraints. We present the results in Appendix F. Qualitatively the results are quite similar to those in Table 8, although the hybrid ZZB and ZZI 6-stencil formulations perform slightly better on these instances, relative to the LogE/LogIB formulations, as compared to when N is a power-of-two. There is no significant difference between the LogE and LogIB 6-stencil formulations.

We also reproduce the computational results from Table 8 using the Gurobi v7.0.2 solver, and include the results in Table 9. The takeaway remains the same, as the new stencil formulations are the fastest performers on every instance in the test bed. Additionally, we observe that, as in the univariate case, Gurobi is generally more efficient than CPLEX on these instances, although the difference between solvers is not nearly as dramatic as on the univariate instances. Additionally,

N	Metric	MC	CC	DLog	6-Stencil +		
					LogE	ZZB	ZZI
4	Mean (s)	1.1	1.8	0.7	0.3	0.3	0.3
	Std	0.8	1.6	0.6	0.1	0.1	0.1
	Win	0	0	0	43	20	37
	Fail	0	0	0	0	0	0
8	Mean (s)	13.0	54.9	12.4	2.1	2.3	2.1
	Std	12.5	79.9	14.8	2.2	2.1	1.9
	Win	0	0	0	52	19	29
	Fail	0	0	0	0	0	0
16	Mean (s)	440.8	1154.9	266.7	16.0	18.7	16.2
	Std	560.9	724.3	438.3	21.1	20.6	18.8
	Win	0	0	0	45	12	23
	Fail	6	39	3	0	0	0
32	Mean (s)	1521.6	1799.0	1291.1	111.6	129.0	121.0
	Std	515.6	-	599.8	145.8	156.6	163.6
	Win	0	0	0	48	10	22
	Fail	56	79	38	0	0	0

Table 9 Computational results with Gurobi for bivariate transportation problems on grids of size $N = d_1 = d_2$.

on the largest instances ($N = 32$), we observe relatively uniform behavior among the three stencil formulation variants, as opposed to CPLEX, for which we observe a substantial relative degradation of the ZZI variant with respect to the other two stencil formulations.

5. Computational tools for piecewise linear modeling: PiecewiseLinearOpt

Throughout this work, we have investigated a number of possible formulations for optimization problems containing piecewise linear functions. The performance of these formulations can be highly dependent on latent structure in the function, and there are potentially a number of formulations one may want to try on a given instance. However, these formulations can seem quite complex and daunting to a practitioner, especially one unfamiliar with the idiosyncrasies of MIP modeling. Anecdotally, we have observed that the complexity of these formulations has driven potential users to simpler but less performant models, or to abandon MIP approaches altogether.

This gap between high-performance and accessibility is fundamental throughout optimization. One essential tool to help close the gap is the modeling language, which allows the user to express an optimization problem in a user-friendly, pseudo-mathematical style, and obviates the need to interact with the underlying optimization solver directly. Because they offer a much more welcoming experience for the modeler, algebraic modeling languages have been widely used for decades, with AMPL (Fourer et al. 1989) and GAMS (Rosenthal 2014) being two particularly storied and

```
using JuMP, PiecewiseLinearOpt, CPLEX
model = Model(solver=CplexSolver())
@variable(model, 0 <= x[1:2] <= 4)
xval = [0,1,2,3,4]
fval = [0,4,7,9,10]
z1 = piecewiselinear(model, x, xval, fval, method=:Log)
g(u,v) = 2*(u-1/3)^2 + 3*(v-4/7)^4
dx = dy = linspace(0, 1, 9)
z2 = piecewiselinear(model, x[1], x[2], dx, dy, g, method=:ZZI)
@objective(model, Min, z1 + z2)
```

Figure 9 PiecewiseLinearOpt code to set the univariate function (1) as the objective, using the LogE formulation.

successful commercial examples. JuMP (Dunning et al. 2017) is a recently developed open-source algebraic modeling language in the Julia programming language (Bezanson et al. 2017) which offers state-of-the-art performance and advanced functionality, and is readily extensible.

To accompany this work, we have created `PiecewiseLinearOpt`, a Julia package that extends JuMP to offer all the formulation options discussed herein through a simple, high-level modeling interface. The package supports continuous univariate piecewise linear functions, and bivariate piecewise linear functions over grid triangulations. It supports all the formulations used in the computational experiments in this work, and can handle the construction and formulation of both structured or unstructured grid triangulations. All this complexity is hidden from the user, who can embed piecewise linear functions in their optimization problem in a single line of code with the `piecewiselinear` function.

In Figure 9, we see sample code for adding piecewise linear functions to JuMP models. After loading the required packages, we define the `Model` object, and add the `x` variables to it. We add the univariate function (1) to our model, specifying it in terms of the breakpoints `xval` of the domain, and the corresponding function values `fval` at these breakpoints. We call the `piecewiselinear` function, while using the LogE formulation. It returns a JuMP variable `z1` which is constrained

to be equal to $f(x)$, and can then be used anywhere in the model, e.g. in the objective function. After this, we add a bivariate piecewise linear function to our model by approximating a nonlinear function g on the box domain $[0,1]^2$. We use the ZZI formulation along each axis x_1 and x_2 ; it will automatically choose the triangulation that best approximates the function values at the centerpoint of each subrectangle in the grid, and then use the 6-stencil triangle selection portion of the formulation, as the triangulation is unstructured.

To showcase the `PiecewiseLinearOpt` package in a more practical setting, we consider a share-of-choice product design problem arising in marketing (e.g. see (Bertsimas and Mišić 2017, Camm et al. 2006, Wang et al. 2009)). We are given a product design space $x \in [0,1]^n$, along with ν customer types, each with a $\lambda_i \in [0,1]$ share of the market and a *partworth* (i.e. preference vector) $\beta^i \in \mathbb{R}^n$. For each customer type i , the probability of purchase is $p_i(x) = \frac{1}{1 + \exp(u_i - \beta^i \cdot x)}$, where u_i is a minimum “utility hurdle” given by existing good products.

Given that the true preference vectors β^i are typically unknown, we may consider a stochastic optimization version of our problem. For each scenario $s \in \llbracket S \rrbracket$, we observe a realized preference vector $\beta^{i,s}$. Our objective is to select the product specification x in order to maximize the expected number of purchases, while ensuring the product performance on each individual realized scenario is not too poor. Mathematically, we may write the optimization problem as

$$\max_{x, \mu, \bar{\mu}, p, \bar{p}} \sum_{i=1}^{\nu} \lambda_i \bar{p}_i \tag{13a}$$

$$\text{s.t. } \bar{\mu}_i = \frac{1}{S} \sum_{s=1}^S \beta^{i,s} \cdot x \quad \forall i \in \llbracket \nu \rrbracket \tag{13b}$$

$$\bar{p}_i = \frac{1}{1 + \exp(u_i - \bar{\mu}_i)} \quad \forall i \in \llbracket \nu \rrbracket \tag{13c}$$

$$\mu_i^s = \beta^{i,s} \cdot x \quad \forall s \in \llbracket S \rrbracket, i \in \llbracket \nu \rrbracket \tag{13d}$$

$$p_i^s = \frac{1}{1 + \exp(u_i - \mu_i^s)} \quad \forall s \in \llbracket S \rrbracket, i \in \llbracket \nu \rrbracket \tag{13e}$$

$$\sum_{i=1}^{\nu} \lambda_i p_i^s \geq C \sum_{i=1}^{\nu} \lambda_i \bar{p}_i \quad \forall s \in \llbracket S \rrbracket \tag{13f}$$

$$0 \leq x_j \leq 1 \quad \forall j \in \llbracket \eta \rrbracket \tag{13g}$$

Metric	Inc	LogE	ZZB	ZZI
Mean (s)	880.9	3600.0	3525.5	776.2
Std	1202.9	-	316.1	1037.1
Win	5	0	0	13
Fail	2	18	17	1

Table 10 Aggregate statistics for share-of-choice problems with 50 piece discretizations.

Here C is some nonnegative scaling constant, and (13f) ensures that the expected number of purchases in a given scenario is not significantly reduced from the overall expected purchases. Our solution approach is to apply a piecewise linear approximation to the nonlinearities arising in (13c) and (13e). This can be easily accomplished with the `PiecewiseLinearOpt` package, as the code in Figure 10 illustrates.

In Table 10 we report the computational performance of high-performing formulations for 18 randomly generated instances of the share-of-choice problem with a $\eta = 15$ dimensional product design space, $\nu = 20$ customer types, $S = 12$ scenarios, scaling constant $C = 0.2$, and $N = 50$ pieces for each piecewise linear discretization. We observe that the ZZI formulation is the best performer on the majority of instances, and substantially outperforms the LogE formulation, which is unable to solve any instance to optimality in 30 minutes or less. Note that for this problem the piecewise linear function will appear in both the objective and the constraints of the optimization problem.

We believe that this exemplifies the value of `PiecewiseLinearOpt`, and modeling languages more generally: it allows a user to quickly and easily write their problem as code, and then iterate as-needed to solve more quickly or to add complexity. For example, we can alter the breakpoint values in the code in Figure 10 to modify the model to produce feasible solutions and upper bounds on the optimal solution. We hope that this simple computational tool will make the advanced formulations available for modeling piecewise linear functions more broadly accessible to researchers and practitioners.

Acknowledgments

This material is based upon work supported by the National Science Foundation under Grant CMMI-1351619.

Endnotes

1. We refer the reader interested in modeling discontinuous functions to Vielma et al. (2010).

```

using JuMP, Distributions, PiecewiseLinearOpt
model = Model()
@variable(model, 0 <= x[1:eta] <= 1)
@variable(model, mu[1:nu, 1:S])
@variable(model, mu_bar[1:nu])
@variable(model, p[1:nu, 1:S])
@variable(model, p_bar[1:nu])
for i in 1:nu
    @constraint(model, mu_bar[i] == 1/S * sum(dot(beta[i,s], x) for s in S))
    f(t) = 1 / (1 + exp(u[i] - t))
    @constraint(model, p_bar[i] == piecewiselinear(model, mu_bar[i], prob_min[i], prob_max[i], f)
    for s in 1:S
        @constraint(model, mu[i,s] == dot(beta[i,s], x))
        @constraint(model, p[i,s] == piecewiselinear(model, mu[i,s], scen_prob_min[i,s], scen_prob_max[i,
            s], f))
    end
end
for s in 1:S
    @constraint(model, sum(lambda[i]*p[i,s] for i in 1:nu) >= C * sum(lambda[i]*p_bar[i] for i in 1:nu))
end
@objective(model, Max, sum(lambda[i]*p_bar[i] for i in 1:nu))

```

Figure 10 PiecewiseLinearOpt code to solve a stochastic share-of-choice problem.

2. To the best of our knowledge, efficient algorithms for certain classes of structured non-bipartite graphs (e.g. the conflict graph of a grid triangulation), have not been investigated in the literature.

References

- Balakrishnan, A., S. C. Graves. 1989. A composite algorithm for a concave-cost network flow problem. *Networks* **19** 175–202.
- Beale, E. M. L., J. A. Tomlin. 1970. Special facilities in a general mathematical programming system for non-convex problems using ordered sets of variables. J. Lawrence, ed., *OR 69: Proceedings of the Fifth International Conference on Operational Research*. Tavistock Publications, 447–454.

-
- Bergamini, M. L., P. Aguirre, I. Grossmann. 2005. Logic-based outer approximation for globally optimal synthesis of process networks. *Computers and Chemical Engineering* **29**(9) 1914–1933.
- Bergamini, M. L., I. Grossmann, N. Scenna, P. Aguirre. 2008. An improved piecewise outer-approximation algorithm for the global optimization of MINLP models involving concave and bilinear terms. *Computers and Chemical Engineering* **32**(3) 477–493.
- Bertsimas, D., V. V. Mišić. 2017. Robust product line design. *Operations Research* **65**(1) 19–37.
- Bezanson, J., A. Edelman, S. Karpinski, V. B. Shah. 2017. Julia: A fresh approach to numerical computing. *SIAM Review* **59**(1) 65–98.
- Bixby, R., E. Rothberg. 2007. Progress in computational mixed integer programming—A look back from the other side of the tipping point. *Annals of Operations Research* **149** 37–41.
- Camm, J. D., J. J. Cochran, D. J. C. an Sriram Kannan. 2006. Conjoint optimization: An exact branch-and-bound algorithm for the share-of-choice problem. *Management Science* **52**(3) 435–447.
- Castro, P. M., J. P. Teles. 2013. Comparison of global optimization algorithms for the design of water-using networks. *Computers and Chemical Engineering* **52** 249–261.
- Codas, A., E. Camponogara. 2012. Mixed-integer linear optimization for optimal lift-gas allocation with well-separator routing. *European Journal of Operational Research* **217**(1) 222–231.
- Codas, A., S. Campos, E. Camponogara, V. Gunnerud, S. Sunjerga. 2012. Integrated production optimization of oil fields with pressure and routing constraints: The Urucu field. *Computers and Chemical Engineering* **46** 178–189.
- Coppersmith, D., J. Lee. 2005. Parsimonious binary-encoding in integer programming. *Discrete Optimization* **2** 190–200.
- Croxtan, K. L., B. Gendron, T. L. Magnanti. 2003. A comparison of mixed-integer programming models for nonconvex piecewise linear cost minimization problems. *Management Science* **49**(9) 1268–1273.
- Croxtan, K. L., B. Gendron, T. L. Magnanti. 2007. Variable disaggregation in network flow problems with piecewise linear costs. *Operations Research* **55**(1) 146–157.
- D’Ambrosio, C., A. Lodi, S. Martello. 2010. Piecewise linear approximation of functions of two variables in MILP models. *Operations Research Letters* **38**(1) 39–46.

- Dantzig, G. B. 1960. On the significance of solving linear programming problems with some integer variables. *Econometrica, Journal of the Econometric Society* 30–44.
- de Farias Jr., I. R., E. Kozyreff, R. Gupta, M. Zhao. 2013. Branch-and-cut for separable piecewise linear optimization and intersection with semi-continuous constraints. *Mathematical Programming Computation* **5**(1) 75–112.
- de Farias Jr., I., M. Zhao, H. Zhao. 2008. A special ordered set approach for optimizing a discontinuous separable piecewise linear function. *Operations Research Letters* **36**(2) 234–238.
- Dunning, I., J. Huchette, M. Lubin. 2017. JuMP: A modeling language for mathematical optimization. *SIAM Review* **59**(2) 295–320.
- Fourer, R., D. M. Gay, B. Kernighan. 1989. *AMPL: a mathematical programming language*. Springer-Verlang.
- Fügenschuh, A., C. Hayn, D. Michaels. 2014. Mixed-integer linear methods for layout-optimization of screening systems in recovered paper production. *Optimization and Engineering* **15** 533–573.
- Garey, M. R., D. S. Johnson. 1979. *Computers and Intractability*. W. H. Freeman and Company.
- Geißler, B., A. Martin, A. Morsi, L. Schewe. 2012. *Using piecewise linear functions for solving MINLPs*. Springer, 287–314.
- Graf, T., P. V. Hentenryck, C. Pradelles-Lasserre, L. Zimmer. 1990. Simulation of hybrid circuits in constraint logic programming. *Computers and Mathematics with Applications* **20**(9–10) 45–56.
- Huchette, J., S. S. Dey, J. P. Vielma. 2017. Strong mixed-integer formulations for the floor layout problem. *INFOR: Information Systems and Operational Research* <https://doi.org/10.1080/03155986.2017.1363592>.
- Huchette, J., J. P. Vielma. 2019a. A combinatorial approach for small and strong formulations of disjunctive constraints. *Mathematics of Operations Research* **44**(3) 767–1144.
- Huchette, J., J. P. Vielma. 2019b. A geometric way to build strong mixed-integer programming formulations <https://arxiv.org/abs/1811.10409>.
- Jeroslow, R. G., J. K. Lowe. 1985. Experimental results on the new techniques for integer programming formulations. *The Journal of the Operational Research Society* **36**(5) 393–403.

-
- Jeroslow, R., J. Lowe. 1984. Modelling with integer variables. *Mathematical Programming Study* **22** 167–184.
- Jeroslow, R. G. 1988. Alternative formulations of mixed integer programs. *Annals of Operations Research* **12** 241–276.
- Jünger, M., T. Liebling, D. Naddef, G. Nemhauser, W. Pulleyblank, G. Reinelt, G. Rinaldi, L. Wolsey. 2010. *50 years of integer programming 1958-2008*. Springer.
- Keha, A. B., I. R. de Farias Jr., G. L. Nemhauser. 2004. Models for representing piecewise linear cost functions. *Operations Research Letters* **32**(1) 44–48.
- Keha, A. B., I. R. de Farias Jr., G. L. Nemhauser. 2006. A branch-and-cut algorithm without binary variables for nonconvex piecewise linear optimization. *Operations Research* **54**(5) 847–858.
- Koch, T., B. Hiller, M. E. Pfetsch, L. Schewe, eds. 2015. *Evaluating Gas Network Capacities*. MOS-SIAM Series on Optimization, SIAM.
- Kolodziej, S., P. M. Castro, I. E. Grossmann. 2013. Global optimization of bilinear programs with a multi-parametric disaggregation technique. *Journal of Global Optimization* **57** 1039–1063.
- Lee, J., D. Skipper, E. Speakman. 2018. Algorithmic and modeling insights via volumetric comparison of polyhedral relaxations. *Mathematical Programming* **170**(1) 121–140.
- Lee, J., D. Wilson. 2001. Polyhedral methods for piecewise-linear functions I: the lambda method. *Discrete Applied Mathematics* **108** 269–285.
- Liu, H., D. Z. Wang. 2015. Global optimization method for network design problem with stochastic user equilibrium. *Transportation Research Part B: Methodological* **72** 20–39.
- Magnanti, T. L., D. Stratila. 2004. Separable concave optimization approximately equals piecewise linear optimization. Daniel Bienstock, George Nemhauser, eds., *Lecture Notes in Computer Science*, vol. 3064. Springer, 234–243.
- Mahlke, D., A. Martin, S. Moritz. 2010. A mixed integer approach for time-dependent gas network optimization. *Optimization Methods and Software* **25**(4) 625–644.
- Markowitz, H. M., A. S. Manne. 1957. On the solution of discrete programming problems. *Econometrica* **25**(1) 84–110.

- Martin, A., M. Möller, S. Moritz. 2006. Mixed integer models for the stationary case of gas network optimization. *Mathematical Programming* **105**(2-3) 563–582.
- Misener, R., C. Floudas. 2012. Global optimization of mixed-integer quadratically-constrained quadratic programs (MIQCQP) through piecewise-linear and edge-concave relaxations. *Mathematical Programming* **136**(1) 155–182.
- Misener, R., C. E. Gounaris, C. A. Floudas. 2009. Global optimization of gas lifting operations: A comparative study of piecewise linear formulations. *Industrial and Engineering Chemistry Research* **48**(13) 6098–6104.
- Misener, R., J. P. Thompson, C. A. Floudas. 2011. APOGEE: Global optimization of standard, generalized, and extended pooling problems via linear and logarithmic partitioning schemes. *Computers and Chemical Engineering* **35** 876–892.
- Muldoon, F. 2012. Polyhedral approximations of quadratic semi-assignment problems, disjunctive programs, and base-2 expansions of integer variables. Ph.D. thesis, Clemson University, Clemson, SC, USA.
- Muldoon, F. M., W. P. Adams, H. D. Sherali. 2013. Ideal representations of lexicographic orderings and base-2 expansions of integer variables. *Operations Research Letters* **41** 32–39.
- Padberg, M. 2000. Approximating separable nonlinear functions via mixed zero-one programs. *Operations Research Letters* **27** 1–5.
- Rebennack, S. 2016. Computing tight bounds via piecewise linear functions through the example of circle cutting problems. *Mathematical Methods of Operations Research* **84** 3–57.
- Rosenthal, R. 2014. *GAMS - A User's Guide*. GAMS Development Corporation.
- Savage, C. 1997. A survey of combinatorial Gray codes. *SIAM Review* **39**(4) 605–629.
- Sherali, H. D., H. Wang. 2001. Global optimization of nonconvex factorable programming problems. *Mathematical Programming* **89**(3) 459–478.
- Silva, T. L., A. Cudas, E. Camponogara. 2012. A computational analysis of convex combination models for multidimensional piecewise-linear approximation in oil production optimization. *Proceedings of the 2012 IFAC Workshop on Automatic Control in Offshore Oil and Gas Production*. 292–298.

-
- Silva, T. L., E. Camponogara. 2014. A computational analysis of multidimensional piecewise-linear models with applications to oil production optimization. *European Journal of Operational Research* **232**(3) 630–642.
- Todd, M. J. 1977. Union Jack triangulations. *Fixed Points: Algorithms and Applications* 315–336.
- Tomlin, J. 1981. A suggested extension of special ordered sets to non-separable non-convex programming problems. *North-Holland Mathematics Studies* **59** 359–370.
- Vielma, J. P. 2015. Mixed integer linear programming formulation techniques. *SIAM Review* **57**(1) 3–57.
- Vielma, J. P. 2018. Embedding formulations and complexity for unions of polyhedra. *Management Science* **64**(10) 4471–4965.
- Vielma, J. P., S. Ahmed, G. Nemhauser. 2010. Mixed-integer models for nonseparable piecewise-linear optimization: Unifying framework and extensions. *Operations Research* **58**(2) 303–315.
- Vielma, J. P., G. Nemhauser. 2011. Modeling disjunctive constraints with a logarithmic number of binary variables and constraints. *Mathematical Programming* **128**(1-2) 49–72.
- Wang, X., F. D. Camm, D. J. Curry. 2009. A branch-and-price approach to the share-of-choice product line design problem. *Management Science* **55**(10) 1718–1728.
- Wilson, D. L. 1998. Polyhedral methods for piecewise-linear functions. Ph.D. thesis, University of Kentucky, Lexington, Kentucky.
- Yildiz, S., J. P. Vielma. 2013. Incremental and encoding formulations for mixed integer programming. *Operations Research Letters* **41** 654–658.

Appendix A: Binary reflected Gray codes, related encodings, and proof of Proposition 3

The following straightforward lemma gives a recursive construction for K^r , C^r , and Z^r .

LEMMA 4. $K^1 = C^1 = Z^1 \stackrel{\text{def}}{=} (0, 1)^T$, and for $r \in \mathbb{N}$ (and $d = 2^r$):

$$K^{r+1} \stackrel{\text{def}}{=} \begin{pmatrix} K^r & \mathbf{0}^d \\ \text{rev}(K^r) & \mathbf{1}^d \end{pmatrix}, \quad C^{r+1} \stackrel{\text{def}}{=} \begin{pmatrix} C^r & \mathbf{0}^d \\ C^r + \mathbf{1}^d \otimes C^r & \mathbf{1}^d \end{pmatrix}, \quad \text{and} \quad Z^{r+1} \stackrel{\text{def}}{=} \begin{pmatrix} Z^r & \mathbf{0}^d \\ Z^r & \mathbf{1}^d \end{pmatrix},$$

where $\mathbf{0}^r, \mathbf{1}^r \in \mathbb{R}^r$ are the vectors with all components equal to 0 or 1, respectively, $u \otimes v = uv^T \in \mathbb{R}^{m \times n}$ for any $u \in \mathbb{R}^m$ and $v \in \mathbb{R}^n$, and $\text{rev}(A)$ reverses the rows of the matrix A .

Proof of Proposition 3 First, we observe that $K^r, Z^r \in \{0, 1\}^{d \times r}$ and that \mathcal{A} is an invertible linear map. Therefore, for each $r \in \mathbb{N}$, K^r , C^r , and Z^r are in convex position. Additionally, as K^r and Z^r are binary matrices, they are trivially hole-free. Additionally, the hole-free property is inherited by C^r from Z^r since \mathcal{A} is invertible and linear, and both \mathcal{A} and \mathcal{A}^{-1} are unimodular ($\mathcal{A}(w) \in \mathbb{Z}^r$ if and only if $w \in \mathbb{Z}^r$).

Now the result is direct from Proposition 2, as $\{c^i \equiv C_{i+1}^r - C_i^r\}_{i=1}^{d-1} = \{\mathbf{e}^k\}_{k=1}^r$, where \mathbf{e}^k is the canonical unit vector with support on component k , and the inverse of \mathcal{A} is $\mathcal{A}^{-1}(y)_k = y_k + \sum_{\ell=k+1}^r 2^{\ell-k-1} y_\ell$ for each $k \in \llbracket r \rrbracket$. Formulations (4) and (5) correspond to encodings C^r and Z^r , respectively. \square

Appendix B: An example where LogE and LogIB do not coincide

Consider the SOS2 instance with $d = 3$ segments. The LogE formulation is all $(\lambda, y) \in \Delta^4 \times \{0, 1\}^2$ such that

$$\lambda_3 + \lambda_4 \leq y_1, \quad \lambda_2 + \lambda_3 + \lambda_4 \geq y_1 \tag{14a}$$

$$\lambda_4 \leq y_2, \quad \lambda_3 + \lambda_4 \geq y_2. \tag{14b}$$

This follows from Proposition 2, after observing that the spanning hyperplanes needed are given by the directions $b^1 = (1, 0)$ and $b^2 = (0, 1)$.

The LogIB formulation is all $(\lambda, y) \in \Delta^4 \times \{0, 1\}^2$ such that

$$\lambda_3 \leq y_1, \quad \lambda_2 + \lambda_3 + \lambda_4 \geq y_1 \tag{15a}$$

$$\lambda_4 \leq y_2, \quad \lambda_3 + \lambda_4 \geq y_2. \tag{15b}$$

This follows from Proposition 4, after observing that a biclique cover for the conflict graph edge set $E = \{\{1, 3\}, \{1, 4\}, \{2, 4\}\}$ is $A^1 = \{3\}$, $B^1 = \{1\}$, $A^2 = \{4\}$, and $B^2 = \{1, 2\}$. We then transform the formulation using the equation $\lambda_1 + \lambda_2 + \lambda_3 + \lambda_4 = 1$ to present the LogIB formulation in a way analogous to (14), where we can observe that the first inequality in (14a) differs from the first inequality in (15a).

Appendix C: 8-segment piecewise linear function formulation branching

Consider the univariate piecewise linear function $f : [0, 8] \rightarrow \mathbb{R}$ given by

$$f(x) = \begin{cases} 8x & 0 \leq x \leq 1 \\ 7x + 1 & 1 \leq x \leq 2 \\ 6x + 3 & 2 \leq x \leq 3 \\ 5x + 6 & 3 \leq x \leq 4 \\ 4x + 10 & 4 \leq x \leq 5 \\ 3x + 15 & 5 \leq x \leq 6 \\ 2x + 21 & 6 \leq x \leq 7 \\ x + 28 & 7 \leq x \leq 8. \end{cases} \quad (16)$$

The corresponding LogIB/LogE formulation is

$$x = \lambda_2 + 2\lambda_3 + 3\lambda_4 + 4\lambda_5 + 5\lambda_6 + 6\lambda_7 + 7\lambda_8 + 8\lambda_9 \quad (17a)$$

$$z = 8\lambda_2 + 15\lambda_3 + 21\lambda_4 + 26\lambda_5 + 30\lambda_6 + 33\lambda_7 + 35\lambda_8 + 36\lambda_9 \quad (17b)$$

$$\lambda_3 + \lambda_7 \leq y_1 \leq \lambda_2 + \lambda_3 + \lambda_4 + \lambda_6 + \lambda_7 + \lambda_8 \quad (17c)$$

$$\lambda_4 + \lambda_5 + \lambda_6 \leq y_2 \leq \lambda_3 + \lambda_4 + \lambda_5 + \lambda_6 + \lambda_7 \quad (17d)$$

$$\lambda_6 + \lambda_7 + \lambda_8 + \lambda_9 \leq y_3 \leq \lambda_5 + \lambda_6 + \lambda_7 + \lambda_8 + \lambda_9 \quad (17e)$$

$$(\lambda, y) \in \Delta^9 \times \{0, 1\}^3, \quad (17f)$$

and the corresponding ZZI formulation is

$$x = \lambda_2 + 2\lambda_3 + 3\lambda_4 + 4\lambda_5 + 5\lambda_6 + 6\lambda_7 + 7\lambda_8 + 8\lambda_9 \quad (18a)$$

$$z = 8\lambda_2 + 15\lambda_3 + 21\lambda_4 + 26\lambda_5 + 30\lambda_6 + 33\lambda_7 + 35\lambda_8 + 36\lambda_9 \quad (18b)$$

$$\lambda_3 + \lambda_4 + 2\lambda_5 + 2\lambda_6 + 3\lambda_7 + 3\lambda_8 + 4\lambda_9 \leq y_1 \leq \lambda_2 + \lambda_3 + 2\lambda_4 + 2\lambda_5 + 3\lambda_6 + 3\lambda_7 + 4\lambda_8 + 4\lambda_9 \quad (18c)$$

$$\lambda_4 + \lambda_5 + \lambda_6 + \lambda_7 + 2\lambda_8 + 2\lambda_9 \leq y_2 \leq \lambda_3 + \lambda_4 + \lambda_5 + \lambda_6 + 2\lambda_7 + 2\lambda_8 + 2\lambda_9 \quad (18d)$$

$$\lambda_6 + \lambda_7 + \lambda_8 + \lambda_9 \leq y_3 \leq \lambda_5 + \lambda_6 + \lambda_7 + \lambda_8 + \lambda_9 \quad (18e)$$

$$(\lambda, y) \in \Delta^9 \times \mathbb{Z}^3 \quad (18f)$$

In Table 11, we show statistics for the relaxations of the both. We observe that the ZZI formulation yields more balanced branching.

Statistic	LogE 0 ↓	LogE 1 ↑	ZZI 0 ↓	ZZI 1 ↑	ZZI 1 ↓	ZZI 2 ↑	ZZI 2 ↓	ZZI 3 ↑	ZZI 3 ↓	ZZI 4 ↑
Volume	41	17	0	38.5	11.5	27	27	11.5	38.5	0
Strengthened Prop.	0	1	1	0.25	0.75	0.5	0.5	0.75	0.25	1

Table 11 Metrics for each possible branching decision on z_1 for LogE and ZZI applied to (16).

Algorithm 2 Computing bicliques that cover anti-diagonal triangle selection edges.

Require: Integer $\tau \in \{0, 1, 2\}$.

```

1: procedure ANTIDIAGONALBICLIQUES( $\tau, E$ )
2:   for  $\kappa \leftarrow \tau, \tau + 3, \dots, d_1 - 1$  do
3:      $\phi \leftarrow \text{true}$ 
4:     for  $j \leftarrow 1, \dots, d_2$  do
5:        $i \leftarrow d_1 + 1 - j - \kappa$ 
6:       if  $1 \leq i \leq d_1$  and  $\{(i, j), (i + 1, j + 1)\} \in E$  then
7:         if  $\phi$  then
8:            $A \leftarrow A \cup (i + 1, j)$ 
9:            $B \leftarrow B \cup (i, j + 1)$ 
10:        else
11:           $A \leftarrow A \cup (i, j + 1)$ 
12:           $B \leftarrow B \cup (i + 1, j)$ 
13:         $\phi \leftarrow \neg \phi$ 
14:    for  $\kappa \leftarrow 3 - \tau, 6 - \tau, \dots, d_2 - 1$  do
15:       $\phi \leftarrow \text{true}$ 
16:      for  $j \leftarrow (1 + \kappa), \dots, d_2$  do
17:         $i \leftarrow d_1 + 1 - j + \kappa$ 
18:        if  $1 \leq i \leq d_1$  and  $\{(i, j), (i + 1, j + 1)\} \in E$  then
19:          if  $\phi$  then
20:             $A \leftarrow A \cup (i + 1, j)$ 
21:             $B \leftarrow B \cup (i, j + 1)$ 
22:          else
23:             $A \leftarrow A \cup (i, j + 1)$ 
24:             $B \leftarrow B \cup (i + 1, j)$ 
25:           $\phi \leftarrow \neg \phi$ 
26:    return  $(A, B)$ 

```

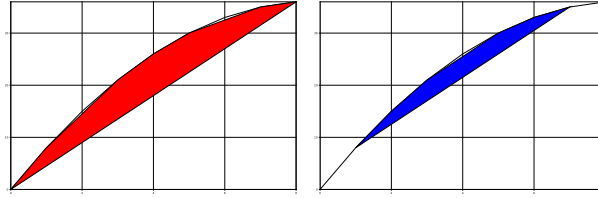


Figure 11 Feasible region in the (x, z) -space for the LogE formulation (17) after: down-branching $y_1 \leq 0$ (left), and up-branching $y_1 \geq 1$ (right).

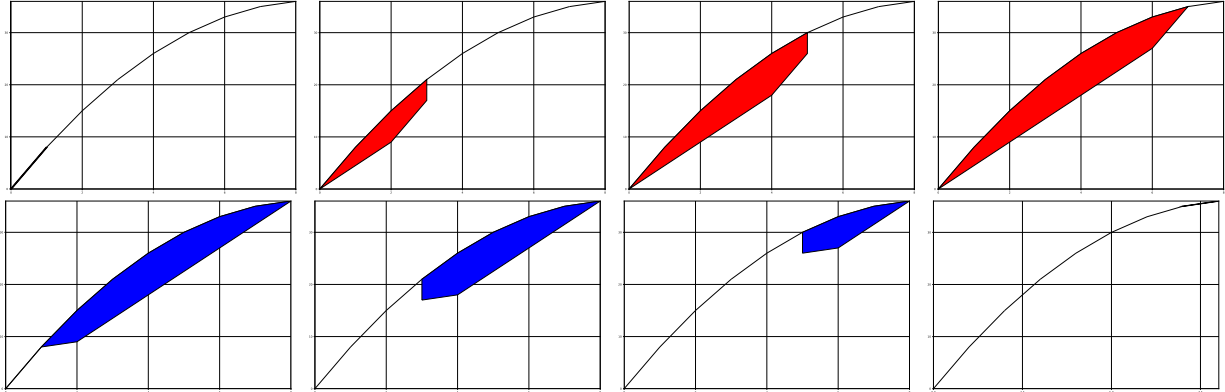


Figure 12 Feasible region in the (x, z) -space for the ZZI formulation (18) after: (Top first column) down-branching on $y_1 \leq 0$, (Bottom first column) up-branching on $y_1 \geq 1$; (Top second column) down-branching on $y_1 \leq 1$, (Bottom second column) up-branching on $y_1 \geq 2$; (Top third column) down-branching on $y_1 \leq 2$, (Bottom third column) up-branching on $y_1 \geq 3$; (Top fourth column) down-branching on $y_1 \leq 3$, and (Bottom fourth column) up-branching on $y_1 \geq 4$.

Appendix D: Algorithm to compute bicliques for anti-diagonal nearby edges

Algorithm 2 presents the analog procedure to Algorithm 1 for the anti-diagonal case.

Appendix E: Proof of Theorem 2

Proof of Theorem 2 For simplicity, assume w.l.o.g. that $V = \llbracket n \rrbracket$. Let

$$\Pi = \left\{ (\lambda, z^1, \dots, z^m) \in \mathbb{R}^{n + \sum_{i=1}^m r_i} \mid (\lambda, z^t) \in \Pi^t \ \forall t \in \llbracket m \rrbracket \right\}$$

be the LP relaxation of (12). Because the original formulations are ideal (and therefore also sharp), we have

$$\text{Proj}_\lambda(\Pi) = \bigcap_{t=1}^m \text{Proj}_\lambda(\Pi^t) = \bigcap_{t=1}^m \text{Conv}(U^t) \subseteq \Delta^n = \text{Conv} \left(\bigcap_{t=1}^m U^t \right),$$

and hence (12) is sharp, as $\text{Proj}_\lambda(\Pi) = \Delta^n$.

To show (12) is also ideal, consider any point $(\hat{\lambda}, \hat{z}^1, \dots, \hat{z}^m) \in \Pi$. First, we show that if this point is extreme, then $\hat{\lambda} = \mathbf{e}^v$ for some $v \in \llbracket n \rrbracket$. Consider some point where $\hat{\lambda}$ is fractional; w.l.o.g.,

presume that $0 < \hat{\lambda}_1, \hat{\lambda}_2 < 1$. Define $\lambda^+ \stackrel{\text{def}}{=} \hat{\lambda} + \epsilon \mathbf{e}^1 - \epsilon \mathbf{e}^2$ and $\lambda^- \stackrel{\text{def}}{=} \hat{\lambda} - \epsilon \mathbf{e}^1 + \epsilon \mathbf{e}^2$ for sufficiently small $\epsilon > 0$; clearly $\hat{\lambda} = \frac{1}{2}\lambda^+ + \frac{1}{2}\lambda^-$. We would like to construct points $z^{t,+}$ and $z^{t,-}$ for each $t \in \llbracket m \rrbracket$ such that $\hat{z}^t = \frac{1}{2}z^{t,+} + \frac{1}{2}z^{t,-}$, and such that $(\lambda^+, z^{t,+}), (\lambda^-, z^{t,-}) \in \Pi^t$. Then $(\hat{\lambda}, \hat{z}^1, \dots, \hat{z}^m) = \frac{1}{2}(\lambda^+, \hat{z}^{1,+}, \dots, \hat{z}^{m,+}) + \frac{1}{2}(\lambda^-, \hat{z}^{1,-}, \dots, \hat{z}^{m,-})$ is the convex combination of two other feasible points for Π , and so is not extreme.

For a given $t \in \llbracket m \rrbracket$, define $E^t = \{(k, h) \mid (\mathbf{e}^k, h) \in \text{ext}(\Pi^t)\}$, which is equivalent to the set of all extreme points of Π^t . As $(\hat{\lambda}, \hat{z}^t) \in \Pi^t$, there must exist some $\gamma^t \in \Delta^{E^t}$ where $(\hat{\lambda}, \hat{z}^t) = \sum_{(k,z) \in E^t} \gamma_{(k,z)}^t (\mathbf{e}^k, h)$. As $1, 2 \in \text{supp}(\hat{\lambda})$, there must exist some \tilde{h}^t and \hat{h}^t wherein $(1, \tilde{h}^t), (2, \hat{h}^t) \in E^t$ and $0 < \gamma_{(1, \tilde{h}^t)}^t, \gamma_{(2, \hat{h}^t)}^t < 1$. Now define

$$\gamma_{(k,h)}^{t,\pm} = \begin{cases} \gamma_{(k,h)}^t \pm \epsilon & k = 1, h = \tilde{h}^t \\ \gamma_{(k,h)}^t \mp \epsilon & k = 2, h = \hat{h}^t \\ \gamma_{(k,h)}^t & \text{o.w.} \end{cases}$$

Note that, as $\gamma^t \in \Delta^{E^t}$, so is $\gamma^{t,\pm} \in \Delta^{E^t}$. Therefore, we may take

$$\begin{aligned} z^{t,+} &\stackrel{\text{def}}{=} \sum_{(k,h) \in E^t} \gamma_{(k,h)}^{t,+} h = \epsilon \tilde{h}^t - \epsilon \hat{h}^t + \sum_{(k,h) \in E^t} \gamma_{(k,h)}^t h \\ z^{t,-} &\stackrel{\text{def}}{=} \sum_{(k,h) \in E^t} \gamma_{(k,h)}^{t,-} h = -\epsilon \tilde{h}^t + \epsilon \hat{h}^t + \sum_{(k,h) \in E^t} \gamma_{(k,h)}^t h. \end{aligned}$$

Then we may observe that $z^{t,+}, z^{t,-} \in \Pi^t$, and that $\hat{z}^t = \frac{1}{2}z^{t,+} + \frac{1}{2}z^{t,-}$. Now see that

$$\lambda^\pm = \sum_{(k,h) \in E^t} \gamma_{(k,h)}^{t,\pm} \mathbf{e}^k = \sum_{(k,h) \in E^t} \gamma_{(k,h)}^t \mathbf{e}^k \pm \epsilon \mathbf{e}^1 \mp \epsilon \mathbf{e}^2 = \hat{\lambda} \pm \epsilon \mathbf{e}^1 \mp \epsilon \mathbf{e}^2$$

Therefore, for each $t \in \llbracket m \rrbracket$, we have that $(\lambda^+, z^{t,+}), (\lambda^-, z^{t,-}) \in \Pi^t$, and that $(\hat{\lambda}, \hat{z}^t) = \frac{1}{2}(\lambda^+, z^{t,+}) + \frac{1}{2}(\lambda^-, z^{t,-})$. This implies that $(\lambda^+, h^{1,+}, \dots, h^{m,+}), (\lambda^+, h^{1,-}, \dots, h^{m,-}) \in \Pi$ and that $(\hat{\lambda}, \hat{z}^1, \dots, \hat{z}^m) = \frac{1}{2}(\lambda^+, h^{1,+}, \dots, h^{m,+}) + \frac{1}{2}(\lambda^-, h^{1,-}, \dots, h^{m,-})$. Therefore, as our original point is a convex combination of two distinct points also feasible for Π , it cannot be extreme. Therefore, we must have that $\lambda = \mathbf{e}^v$ for some $v \in \llbracket n \rrbracket$ for any extreme point of Π .

Now, assume for contradiction that Π has a fractional extreme point. Using property of extreme points just stated, we may assume without loss of generality that this fractional extreme point is of the form $(\mathbf{e}^1, \hat{z}^1, \dots, \hat{z}^m)$ with $\hat{z}^1 \notin \mathbb{Z}^{r_1}$. As $(\mathbf{e}^1, \hat{z}^1) \in \Pi^1$, then $(\mathbf{e}^1, \hat{z}^1) = \sum_{(v,h) \in E^1} \gamma_{(v,h)} (\mathbf{e}^v, h)$ for some $\gamma \in \Delta^{E^1}$. Also, as Π^1 is ideal and \hat{z}^1 is fractional, $(\mathbf{e}^1, \hat{z}^1) \notin \text{ext}(\text{Conv}(\Pi^1))$, and so γ must have at least two non-zero components. But then

$$(\hat{\lambda}, \hat{z}^1, \hat{z}^2, \dots, \hat{z}^m) = \sum_{(v,h) \in E^1} \gamma_{(v,h)} (\mathbf{e}^1, h, \hat{z}^2, \dots, \hat{z}^m),$$

a contradiction of the points extremality. Therefore, Π is ideal. \square

Appendix F: Non-power-of-two bivariate computational results

See Table 12.

N	Metric	MC	CC	DLog	LogE	LogIB	ZZB	ZZI
6	Mean (s)	9.2	20.8	4.7	1.2	1.5	1.5	1.1
	Std	12.0	33.0	3.4	0.7	1.1	1.2	0.6
	Win	0	0	0	31	9	12	48
	Fail	0	0	0	0	0	0	0
13	Mean (s)	1092.9	1507.9	320.3	16.8	16.5	17.3	18.1
	Std	729.7	535.4	478.7	18.6	15.7	18.6	19.3
	Win	0	0	0	16	26	23	15
	Fail	37	58	4	0	0	0	0
28	Mean (s)	1768.1	1800.0	1426.2	127.3	131.2	113.4	192.7
	Std	139.6	-	513.5	174.5	188.7	129.7	254.9
	Win	0	0	0	20	26	31	3
	Fail	75	80	46	0	0	0	0

Table 12 Computational results for transportation problems whose objective function is the sum of bivariate piecewise linear objective functions on grids of size $N = d_1 = d_2$, when N is not a power-of-two.